



NATO Undersea Research Centre
Centre de Recherche Sous-Marine de l'OTAN



Reprint Series

NURC-PR-2006-029

Design of synthetic aperture sonar systems for high-resolution seabed imaging (tutorial slides)

Marc Pinto

October 2006

Originally presented as a tutorial at :

OCEANS'06 MTS/IEEE Boston, Massachusetts, USA, 18-21 September
2006

NATO Undersea Research Centre (NURC)

NURC conducts world class maritime research in support of NATO's operational and transformational requirements. Reporting to the Supreme Allied Commander Transformation, the Centre maintains extensive partnering to expand its research output, promote maritime innovation and foster more rapid implementation of research products.

The Scientific Programme of Work (SPOW) is the core of the Centre's activities and is organized into four Research Thrust Areas:

- Expeditionary Mine Countermeasures (MCM) and Port Protection (EMP)
- Reconnaissance, Surveillance and Undersea Networks (RSN)
- Expeditionary Operations Support (EOS)
- Command and Operational Support (COS)

NURC also provides services to other sponsors through the Supplementary Work Program (SWP). These activities are undertaken to accelerate implementation of new military capabilities for NATO and the Nations, to provide assistance to the Nations, and to ensure that the Centre's maritime capabilities are sustained in a fully productive and economic manner. Examples of supplementary work include ship chartering, military experimentation, collaborative work with or services to Nations and industry.

NURC's plans and operations are extensively and regularly reviewed by outside bodies including peer review of the research, independent national expert oversight, review of proposed deliverables by military user authorities, and independent business process certification. The Scientific Committee of National Representatives, membership of which is open to all NATO nations, provides scientific guidance to the Centre and the Supreme Allied Commander Transformation.



Copyright © NATO Undersea Research Centre 2005. NATO member nations have unlimited rights to use, modify, reproduce, release, perform, display or disclose these materials, and to authorize others to do so for government purposes. Any reproductions marked with this legend must also reproduce these markings. All other rights and uses except those permitted by copyright law are reserved by the copyright owner.

NOTE: The NURC Reprint series reprints papers and articles published by NURC authors in the open literature as an effort to widely disseminate NURC products. Users are encouraged to cite the original article where possible.

Design of synthetic aperture sonar systems for high-resolution seabed imaging

Editorial Note:

This reprint is a compilation of the slides presented at the OCEANS'06 tutorial of the same title above.

Summary of the tutorial

This tutorial reviews the key aspects of the design of synthetic aperture sonar (SAS) systems for high resolution seabed imaging. After a quick overview of the expected benefits and main features of SAS, the design of the transmitter and receiver arrays is discussed, with emphasis on the mitigation of spatial aliasing with multi-element receiver arrays, wideband operation and extension to interferometric SAS for estimating the seabed bathymetry. The most difficult issue in SAS, which is the micronavigation problem, i.e. estimating the unwanted platform motions with the required sub-wavelength accuracy, will be addressed in detail. The emphasis is on methods that have proven their value at sea, which combine inertial navigation systems (INS) with data-driven methods based on the Displaced Phase Centre Antenna (DPCA) technique.

The topics covered include:

- the theory of spatial backscatter coherence,
- the derivation of ping to ping motion estimates using time delay estimation theory, including the use of bandwidth for phase unwrapping and the appropriate range-dependent near field corrections to arrive at unbiased estimates,
- the establishment of the Cramer Rao lower bounds for motion estimation which demonstrate the need for fusion with an INS to achieve full performance.

The geometrical relationship between the DPCA and INS projection frames, which is necessary for accurate fusion, will be established and shown to depend also on the local seabed slope. The estimation of this slope with interferometric sonar is discussed. Furthermore the impact of the environment, and in particular of the multipath structure in large range to water depth ratios is discussed. Multipath is shown to degrade the quality of the SAS imagery as well as adversely impact the accuracy of interferometric estimates including DPCA. Means to mitigate multipath operation by management of the vertical transmission and reception beams is discussed, showing experimental results which point to some of the limitations of existing sonar performance prediction tools.

Finally different design trade-offs between computational efficiency and robustness for micronavigated SAS imaging algorithms is discussed, and an example of a real-time implementation suited for operation on-board an autonomous underwater vehicle will be described.

About the presenter

Marc Pinto was born in Wellington, India in 1960. He graduated from the Ecole Nationale des Ponts et Chaussées, Paris (France) in 1983. From 1985 to 1989 and 1989 to 1993 he worked as a research engineer for Thomson-CSF, specializing in the development of finite element techniques for solving non-linear magnetostatics to support the modeling of the magnetic recording process. In 1991, he received the Ph.D. degree in Solid State Physics from the University of Paris, Orsay. In 1993 he joined Thomson-Sintra ASM (now Thales Underwater Systems) as Head of the Signal Processing Group, specializing in research into advanced MCM and airborne ASW sonar.

Dr Pinto joined the NATO Saclant Undersea Research Center, La Spezia, Italy in 1997 as principal scientist. He was appointed Head of the Mine Countermeasures Group, in the Signal and Systems Division in 1998 and held this position until the Group was dissolved in 2000. From 2000 to 2004, as project leader, he conducted research into synthetic aperture sonar systems for hunting proud and buried mines. In 2004 he was appointed Head of the Expeditionary MCM and Port Protection Department where he presently oversees the research into AUV-based minehunting, electronic mine countermeasures and harbour defence.



NATO
OTAN

NATO Undersea Research Centre
Partnering for Maritime Innovation



NURC

Synthetic Aperture Sonar Tutorial

Marc Pinto
NATO Undersea Research Centre



Overview



I. SAS array design

II. SAS micronavigation

III. Impact of the shallow water environment on SAS

IV. Applications

Tutorial presented at Oceans'06 © NURC

1




1. SAS array design

- Benefit of SAS for high resolution imaging
- Single-element SAS
 - SAS beamforming: principle & examples
 - Ambiguities & spatial sampling
 - Relation to Doppler processing
- Phase Centre Approximation
- Multi-element SAS design
- Multi-aspect SAS

Tutorial presented at Oceans'06 © NURC

2




Benefit of SAS

- Today's technology offers very high range resolution using wideband pulses:

$$RR = \frac{c}{2B}$$
- High cross-range resolution (CRR) is difficult to obtain with real aperture sonar (RAS):

$$CRR = \frac{\lambda}{L} r$$

 - Sound absorption set the limit on minimum λ .
 - Platform size sets the limit on maximum L .
 - CRR increases with range r .
- SAS will allow CRR independent of λ & r with practical platform sizes.
- It increases the options for the sonar designer but is not always the best option.

Tutorial presented at Oceans'06 © NURC

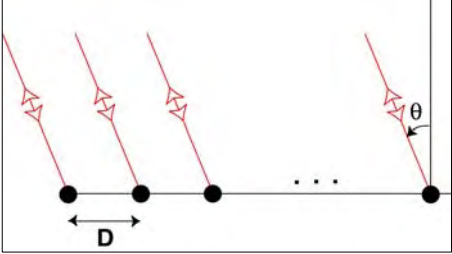
3



Single-element SAS



- Obtained by displacing a single transducer.
- Virtual array sampled at the ping-to-ping displacement D .



- The ping-to-ping phase shift is twice that of a RAS

$$\Delta\phi = \frac{4\pi}{\lambda} D \sin \theta$$

- The SAS beampattern is the same as that of a RAS with element spacing $2D$ or wavelength $\lambda/2$.

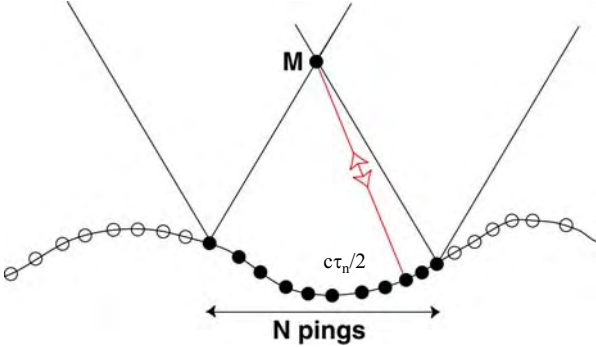
Tutorial presented at Oceans'06 © NURC

4



SESAS image formation (elementary backprojection approach)





- Compute two-way travel times τ_n to M for all N pings in the SAS
- Temporal interpolation of the sonar returns and coherent summation:

$$I(M) = \left| \sum_{n=1}^N X_n(\tau_n) \right|^2$$

Tutorial presented at Oceans'06 © NURC

5




Relation to Doppler processing

- The ping to ping changes in round-trip travel time are often interpreted in SAR as resulting from a Doppler effect.

$$f_d = \frac{1}{2\pi} \frac{\Delta\phi}{PRP} = \frac{2v}{\lambda} \sin \theta$$

- The corresponding Doppler processing is mathematically equivalent to SAS beamforming.
- The above must not be confused for the Doppler effect resulting from travel time changes during the pulse length.

Tutorial presented at Oceans'06 © NURC 6




Cross-range resolution of SAS

- The SAS length is defined by two-way physical transducer 4-dB beam pattern:

$$L_{SAS} = \frac{\lambda}{L} r$$

- The CRR is

$$CRR = \frac{\lambda}{2L_{SAS}} r = \frac{L}{2}$$

CRR is independent of range & frequency and decreases with L.

Tutorial presented at Oceans'06 © NURC 7



SAS ambiguities



- Range ambiguities are avoided provided

$$PRP \geq \frac{2R_{\max}}{c}$$

- Azimuth ambiguities are due to the SAS grating lobes which are spaced at $\lambda/2D$ when $D > \lambda/4$. They lead to ghost targets and loss of image contrast.
- Their reduction increases with the SAS oversampling factor:

$$OSF = \frac{L}{2D} \geq 1$$

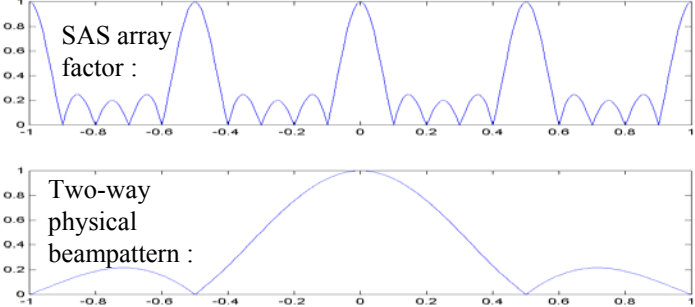
Tutorial presented at Oceans'06 © NURC
8



Pattern multiplication paradox

(Why OSF=1 is not enough...)





$$\frac{\sin(Nu)}{N \sin(u)} \cdot \frac{\sin(u)}{u} = \frac{\sin(Nu)}{Nu}$$

$$u = \frac{4\pi}{\lambda} D \sin \theta = \frac{2\pi}{\lambda} L \sin \theta$$

But the pattern multiplication rule applies only in SAS far field !!

Tutorial presented at Oceans'06 © NURC
9

Solution to the paradox

The diagram shows a vertical axis with an upward arrow. A horizontal line represents the SAS length, with a double-headed arrow labeled $\lambda R/2L$ below it. A black dot is on the vertical axis above the center of the SAS length. A horizontal double-headed arrow labeled $\lambda R/2D$ is positioned above the black dot. A ghost target, represented by a black dot, is located on the vertical axis above the mainlobe. The mainlobe is a yellow-to-orange gradient inverted triangle with its apex at the center of the SAS length. Two small circles are on the upper edges of the mainlobe. The text "ghost target" is to the right of the black dot on the vertical axis.

Ghost targets are in nulls of RAS only at the SAS centre.
At the extremities of the SAS they move into the mainlobe.

Tutorial presented at Oceans'06 © NURC

10

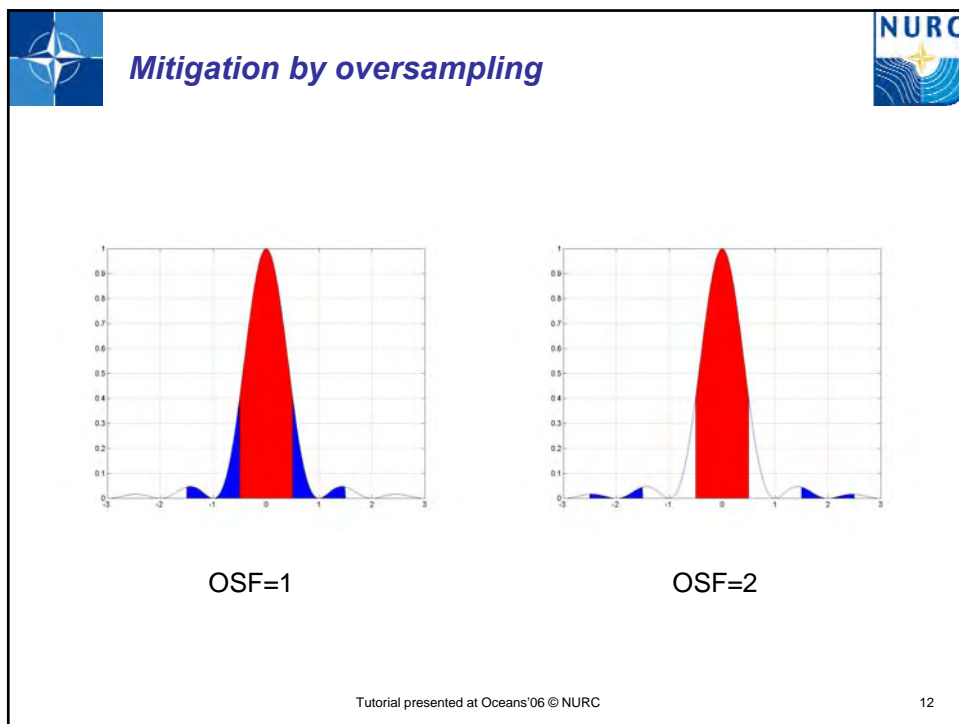
Solution to the paradox

The diagram is similar to the one above, but the ghost target (black dot) is now located within the mainlobe. Two thin lines extend from the apex of the mainlobe to the two small circles on its edges. The text "ghost target" is to the right of the black dot on the vertical axis.

Ghost targets are in nulls of RAS only at the SAS centre.
At the extremities of the SAS they move into the mainlobe.

Tutorial presented at Oceans'06 © NURC

11



Area mapping rate

- The ping-to-ping displacement determines the area mapping rate AMR defined as

$$AMR = vR_{\max} = v \frac{c}{2} PRP = \frac{c}{2} D = \frac{cL}{8}$$

- OSF=2 is assumed above.
- Therefore long physical apertures are required to achieve high AMR

Tutorial presented at Oceans'06 © NURC

13




Summary for SESAS

- SESAS is characterized by a tradeoff between AMR and image quality (resolution and contrast) which severely limits its applicability.

$$CRR = \frac{L}{2} \quad D = \frac{L}{4} = \frac{CRR}{2}$$

- In order words, to achieve high resolution at any reasonable range requires going unreasonably slow !
- Example of SESAS design: R=150 m, CRR=2.5cm, => v=6.25cm/s!
- SESAS is essentially of academic interest, to facilitate the understanding of the multi-element SAS (MESAS) which is used in most if not all sonar applications.

Tutorial presented at Oceans'06 © NURC 14




Multi-element SAS (MESAS) design

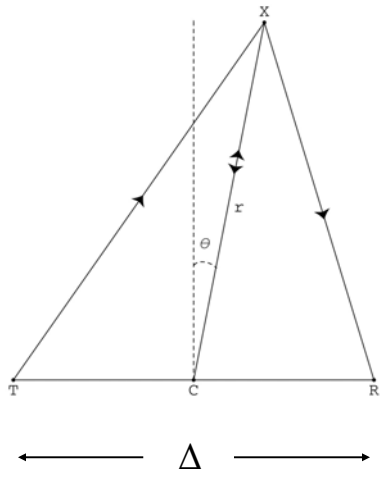
- The multi-element SAS design consists of different transmitter and receiver arrays to decouple conflicting requirements on CRR and AMR.
- Typical design is a
 - broad sector transmitter whose length L_t is determined by the desired CRR.
 - a multi-element receiver array of N elements of length $d < L_t$ where N is determined by the desired AMR.

Tutorial presented at Oceans'06 © NURC 15



Phase Centre Approximation





- In far field, transmission at T and reception at R is equivalent to transmission & reception at C.
- This also holds in near field provided the signal is advanced by

$$\tau = \frac{\Delta^2}{4rc}$$

and

$$\frac{\Delta^2}{4r} (1 - \cos^2 \theta_e) \ll \lambda$$

Tutorial presented at Oceans'06 © NURC

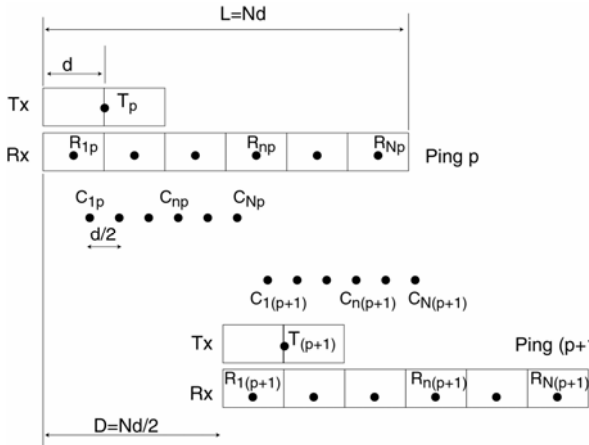
16



Multi-element SAS design



- The MESAS is equivalent to a SESAS made up by the phase centres and ping to ping displacement $D_1 = d/2$.



Tutorial presented at Oceans'06 © NURC

17




MESAS design criteria

- AMR increases with receive array length L_r independently of image quality (contrast or resolution)

$$AMR_N = \frac{cL_r}{4}$$
- CRR improves with decreasing transmitter length L_t independently from AMR.

$$CRR_N = \frac{L_t}{2}$$
- Higher spatial sampling d of the receive array improves image quality

$$OSF = \frac{L_t}{d}$$

Tutorial presented at Oceans'06 © NURC 18




MESAS image formation (factorized backprojection approach)

- The elementary SESAS approach can be accelerated by using an intermediate stage of beamforming of the physical array.
- Since the physical array is linear equispaced fast beamforming techniques can be used.
- The physical beams are then interpolated in angle and time and summed over the P pings of the SAS.

$$I(M) = \left| \sum_{p=1}^P W_p(\theta_p, \tau_p) \right|^2$$

Tutorial presented at Oceans'06 © NURC 19




MESAS design example

- *SESAS* : $R=150$ m, $v=2$ m/s, $OSF=2$ \Rightarrow $L=1.6$ m, $CRR=0.8$ m.
- *Benefit of MESAS*: $R=150$ m, $v=2$ m/s, $OSF=2$, $CRR=5$ cm, \Rightarrow $L_r=0.8$ m, $L_t=10$ cm, $d=5$ cm, $N=16$.
- *Example of long range MESAS*: $R=500$ m, $v=2$ m/s, $OSF=2$, $CRR=5$ cm, \Rightarrow $L_r=2.7$ m, $L_t=10$ cm, $d=5$ cm, $N=54$.
- Joined optimisation of the placement of transmission and receive element nulls can allow to reduce $OSF=1.5$.
- High performance SAS comes at the price of increased size and complexity of the physical array since many elements are required.

Tutorial presented at Oceans'06 © NURC

20




Alternatives to MESAS

- Are there any alternatives to the complex MESAS design?
- Many ideas (and patents) proposed based on
 - Multiple transmitters,
 - Multiple frequencies,
 - Multiple transmission waveforms
 - Combinations of the above
- In most cases there is a price to pay in terms of image quality with respect to the MESAS solution.
- The loss in image quality is basically that of an undersampled MESAS.

Tutorial presented at Oceans'06 © NURC

21



II. SAS micronavigation



- I. Purpose
- II. DPCA micronavigation
- III. DPCA micronavigation accuracy
- IV. Experimental results
- V. Fusion with Inertial Navigation Sensors
- VI. Effect of the environment on DPCA

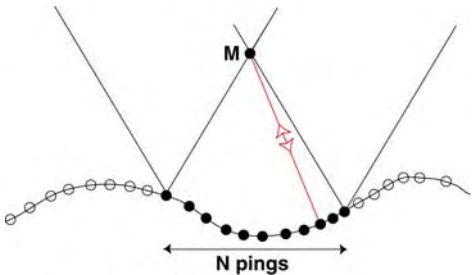
Tutorial presented at Oceans'06 © NURC

22



Purpose of micronavigation





- Travel time errors result from errors in motion sensing of the sonar displacement, leading to image defocusing & distortion, and inaccurate geo-referencing.
- Line-of-sight (LOS) motion must be known with sub-wavelength accuracy (within $\lambda/16$ for random errors).
- Motion sensing errors must not be confused with track-keeping errors !!

Tutorial presented at Oceans'06 © NURC

23



Relation to SAR terminology



- Platform motion sensing using inertial navigation sensors is used in airborne SAR. The ratio of the track-keeping errors to the motion sensing errors is known as the “motion compensation” ratio.
- Additional data-driven techniques, known as “autofocusing” are used to compensate for inertial errors in LOS. They typically assume the presence of point-like targets in the field of view.
- Micronavigation is used as motion sensing with the accuracy required to focus the SAS. It will in general combine inertial instrumentation with data-driven techniques which typically do not assume presence of point-targets.

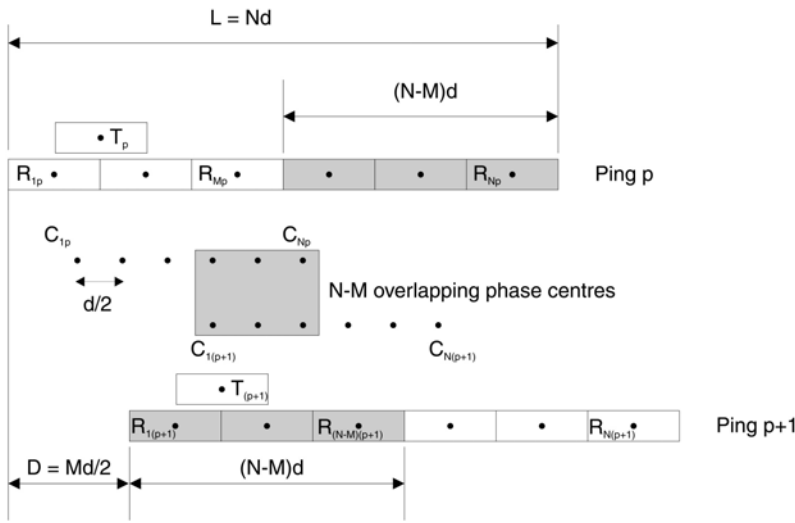
Tutorial presented at Oceans'06 © NURC

24



Displaced Phase Centre Antenna





The diagram illustrates the geometry of a Displaced Phase Centre Antenna. It shows two ping configurations, Ping p and Ping p+1, along a horizontal axis.

- Ping p:** A horizontal line representing the range gate. The total length is $L = Nd$. The range gate is divided into segments of length d . The first segment is labeled R_{1p} and the last segment is R_{Np} . A target T_p is located at the center of the first segment. The distance from the center of the range gate to the target is $(N-M)d$.
- Ping p+1:** A horizontal line representing the range gate. The total length is $D = Md/2$. The range gate is divided into segments of length d . The first segment is labeled $R_{1(p+1)}$ and the last segment is $R_{N(p+1)}$. A target $T_{(p+1)}$ is located at the center of the first segment. The distance from the center of the range gate to the target is $(N-M)d$.
- Phase Centers:** A central shaded rectangle represents the antenna array. The phase centers are labeled C_{1p} , C_{Np} , $C_{1(p+1)}$, and $C_{N(p+1)}$. The distance between C_{1p} and C_{Np} is $d/2$. The text "N-M overlapping phase centres" is placed between the two ping configurations.

Tutorial presented at Oceans'06 © NURC

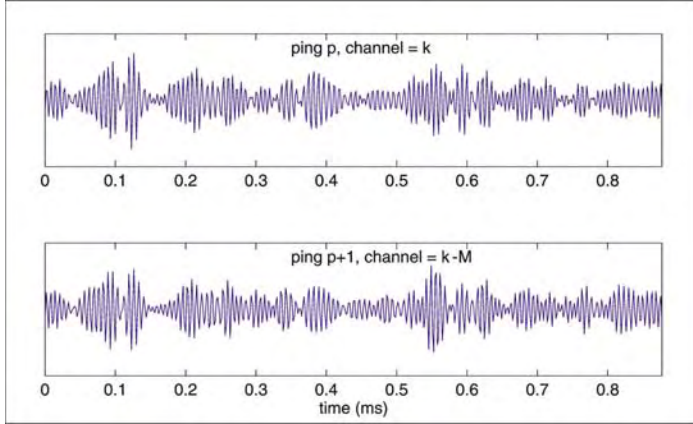
25



Waveform invariance



➤ The reverberation signals of Rx channels with overlapped phase centres have maximum correlation

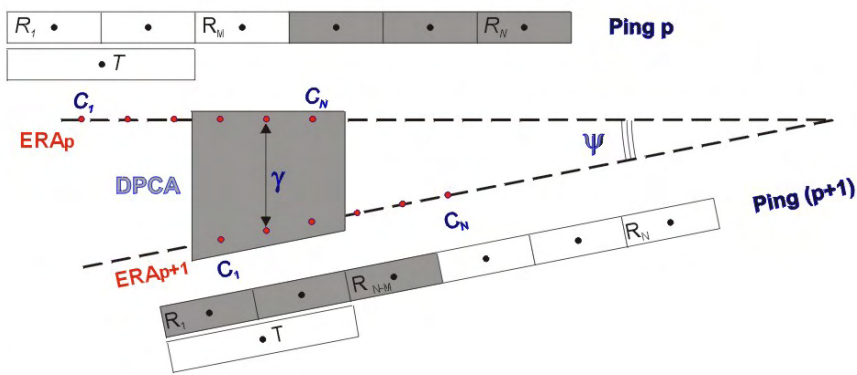


Tutorial presented at Oceans'06 © NURC 26



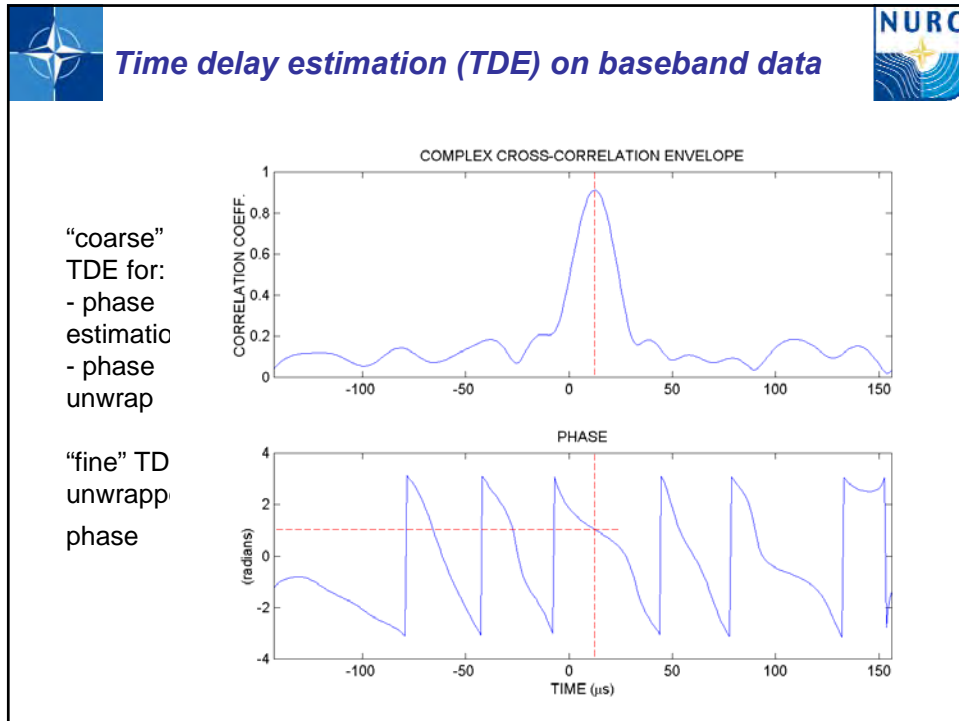
DPCA ping to-ping estimation





The often-used terminology of sway and yaw is somewhat improper. Sway refers to a component of the motion projected in the slant range plane and Yaw to the same projection of the change in the array heading.

Tutorial presented at Oceans'06 © NURC 27



Cramer Rao Lower Bound (CRLB) on time delay estimate

$$\sigma_{\tau} = \frac{1}{2\pi f_0} \frac{1}{\sqrt{BW}} \sqrt{\frac{1 - \mu^2}{2\mu^2}}$$

- where B is bandwidth,
- W is correlation window length
- μ is the correlation coefficient, which depends on the reverberation to noise ratio

$$\mu = \frac{\rho}{1 + \rho}$$

Tutorial presented at Oceans'06 © NURC

29



CRLBs on DPCA sway & yaw



$$\sigma_\gamma \approx \frac{\lambda}{4\pi} \sqrt{\frac{\alpha}{\alpha-1}} \frac{1}{\sqrt{\rho_{eff}}}$$

$$\alpha = \frac{L}{2D}$$

$$\sigma_\psi \approx \frac{\sqrt{3}}{\pi} \frac{\lambda}{L} \sqrt{\frac{\alpha^3}{(\alpha-1)^3}} \frac{1}{\sqrt{\rho_{eff}}}$$

$$\rho_{eff} \approx NBW\rho$$

- The sway (resp. yaw) standard deviation decreases with α .
- Their value for big α is limited by ρ_{eff} and λ (resp. λL).

Tutorial presented at Oceans'06 © NURC

30



Experimental validation of CRLB



Tutorial presented at Oceans'06 © NURC

31



DPCA micronavigation error analysis



- Ping-to-ping motion estimates have to be integrated along the SAS.
- DPCA errors accumulate leading to an integrated random walk of the cross-track errors. Thus the accuracy requirement becomes increasingly challenging as the SAS length increases. Ultimately this is what will limit the achievable SAS performance.
- The most important errors are not the errors on the sway estimates themselves but projection errors induced by errors in estimation the heading of the physical array.

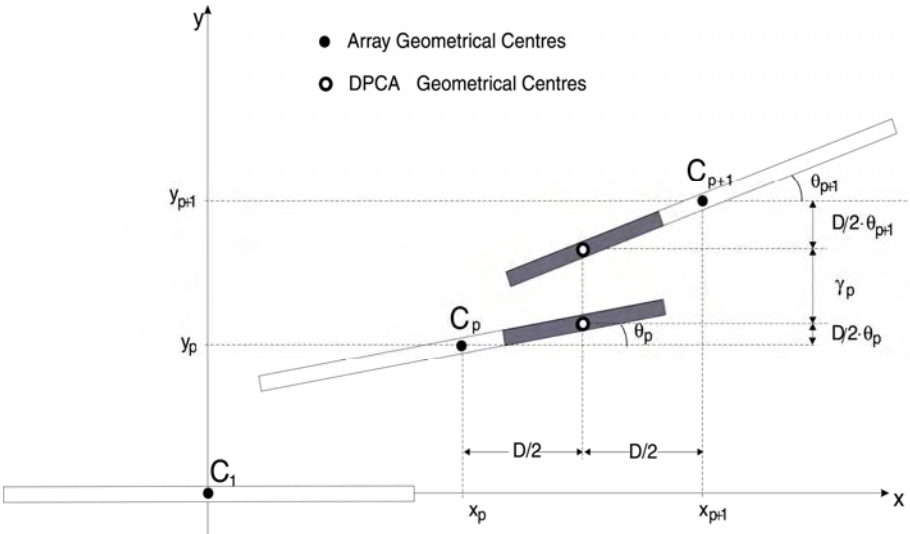
Tutorial presented at Oceans'06 © NURC

32



Error accumulation in DPCA micronavigation





Tutorial presented at Oceans'06 © NURC

33



Performance metrics for DPCA-micro-navigated SAS



➤ Loss in SAS array gain is a simple metric to quantify loss in SAS imaging quality due to micronavigation errors.

$$G = \frac{1}{P^2} \left\langle \left| \sum_{p=1, \dots, P} e^{j\phi_p} \right|^2 \right\rangle$$

$$\phi_p = \frac{4\pi}{\lambda} \delta y_p$$

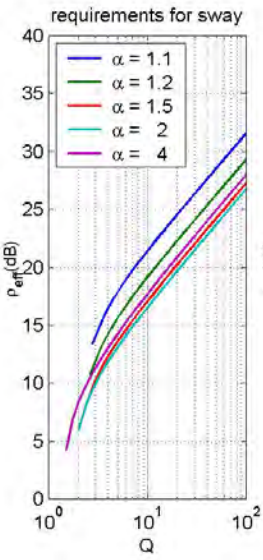
Tutorial presented at Oceans'06 © NURC
34



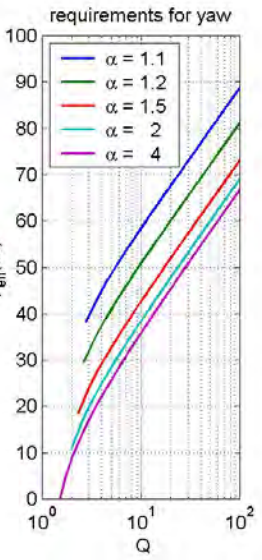
Optimum DPCA performance



requirements for sway



requirements for yaw



➤ The build up of DPCA errors limits the number of pings P in the SAS, hence the SAS resolution gain

$$Q = 1 + \frac{P-1}{\alpha}$$

➤ DPCA accuracy is dominated by yaw accuracy requirements.

➤ Practical optimum is $\alpha \approx 2$.

Tutorial presented at Oceans'06 © NURC
35



DPCA-micronavigated SAS design



- The higher spatial sampling required for DPCA limits the area mapping rate achievable by DPCA micronavigated SAS.
- The use of DPCA for yaw estimation practically limits the resolution gain Q of the SAS to less than 10 for $\alpha=2$.
- *Example of SAS design $R=150\text{ m}$, $v=2\text{ m/s}$, $OSF=2$, $CRR=5\text{ cm}$, $\alpha=2 \Rightarrow L_r=1.6\text{ m}$, $L_t=10\text{ cm}$, $d=5\text{ cm}$, $N=16$. This is compatible with an operating frequency of $f_0=400\text{ kHz}$ since the required Q is only 7.*

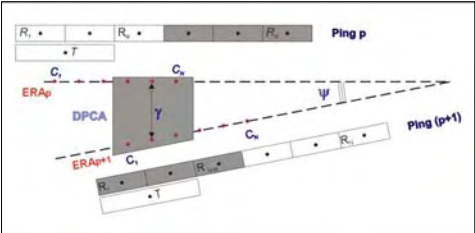
Tutorial presented at Oceans'06 © NURC

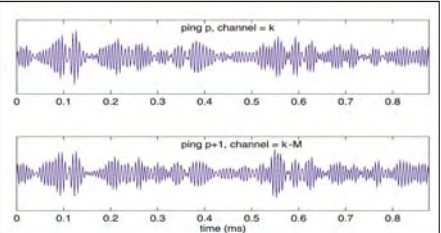
36



Integrated navigation









Wideband sonar

DPCA concept



Inertial navigation

Optimal fusion by Kalman filter

Tutorial presented at Oceans'06 © NURC

37



Gyro-stabilized DPCA



- Gyro-stabilized DPCA is an rudimentary way to implement integrated navigation.
- The idea is to sense the heading changes of the physical array using inertial gyroscopes.
- The accuracy requirement for these gyroscopes is modest due to the short SAS integration time compared to typical mission times.
- Knowledge of local grazing angle is necessary to project inertial estimates in slant range plane. This can be provided by an interferometric sonar.
- G-DPCA should allow a significant increase in both SAS mapping rate ($\alpha=1.3$) and resolution ($Q=20-30$).

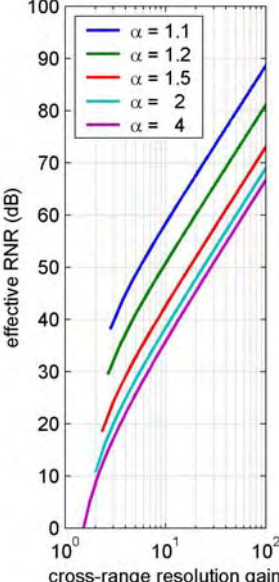
Tutorial presented at Oceans'06 © NURC 38



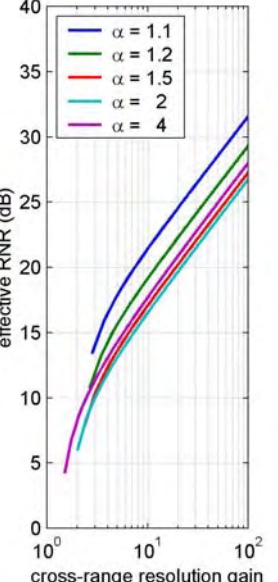
Theoretical Accuracy G-DPCA vs DPCA.



DPCA



gyro-stabilized DPCA



DPCA

$$\div Q^3 \frac{\alpha^4}{(\alpha - 1)^3}$$

Gyro-stabilized DPCA

$$\div Q \frac{\alpha^2}{\alpha - 1}$$

- 0.25 dB array gain loss

39



INSAS'00 Experiment

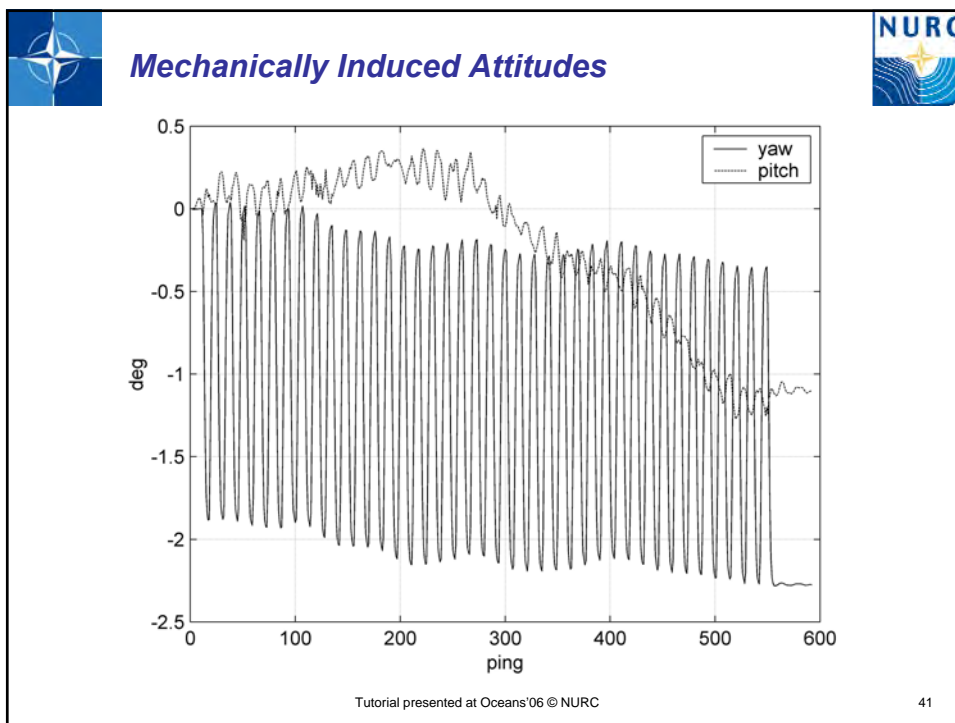


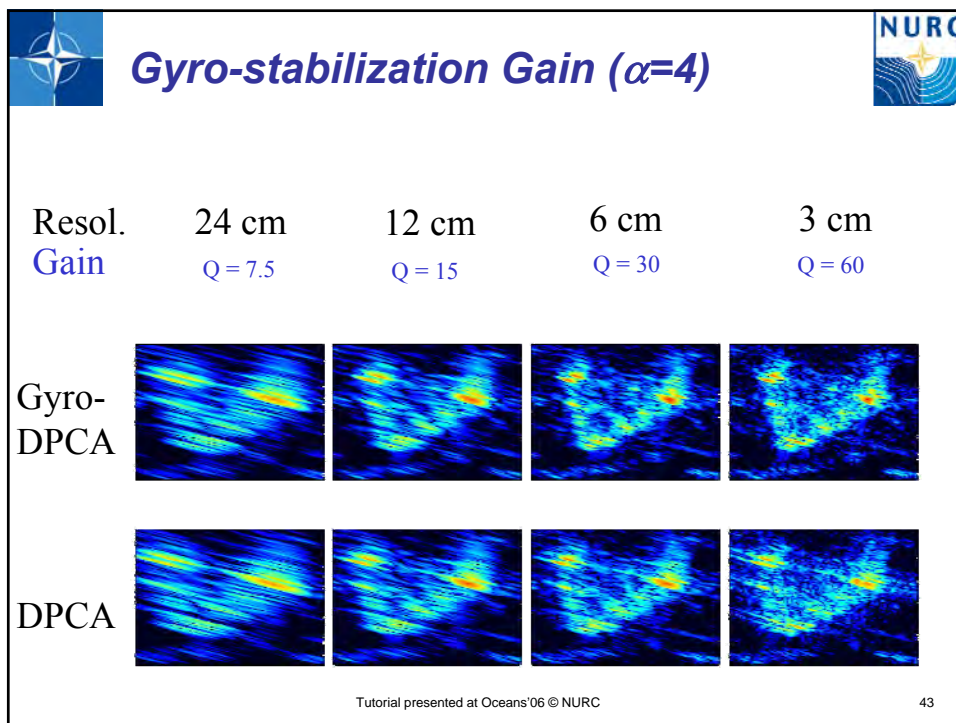
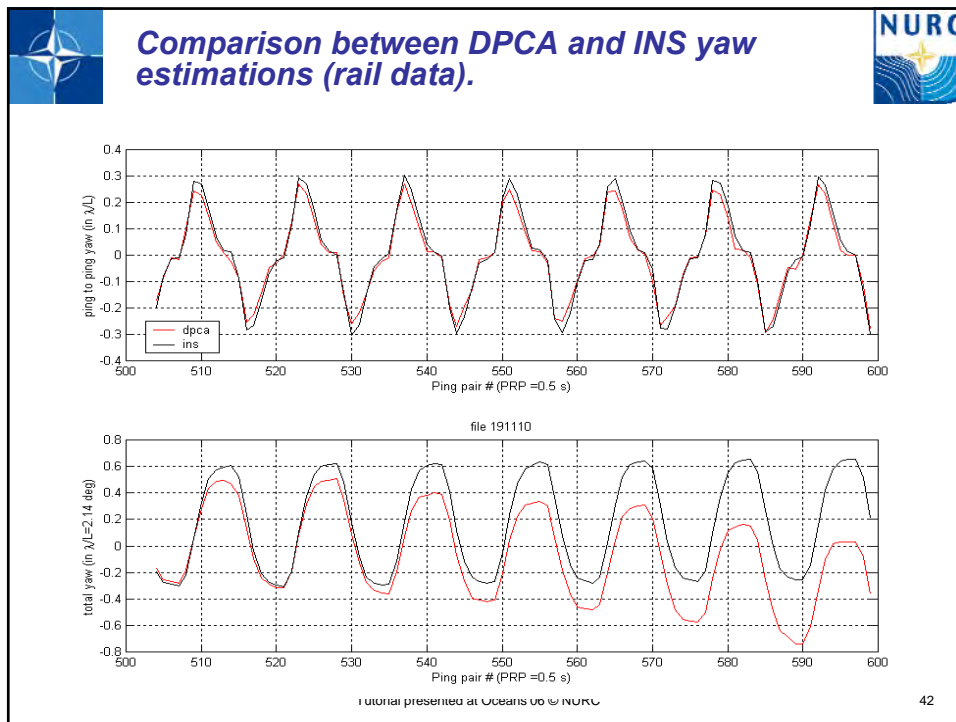


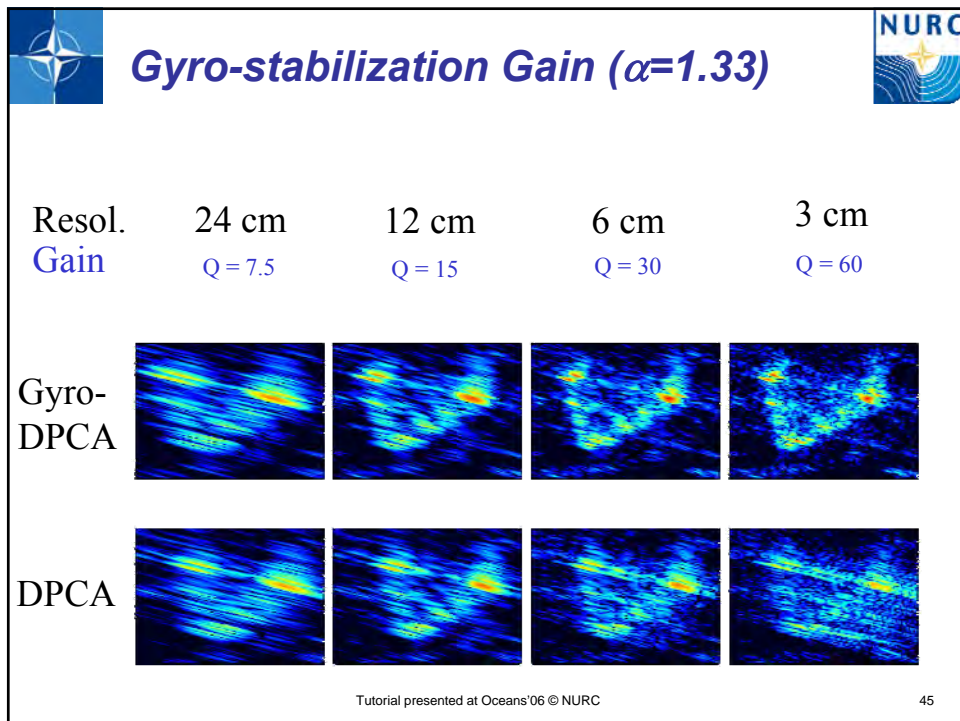
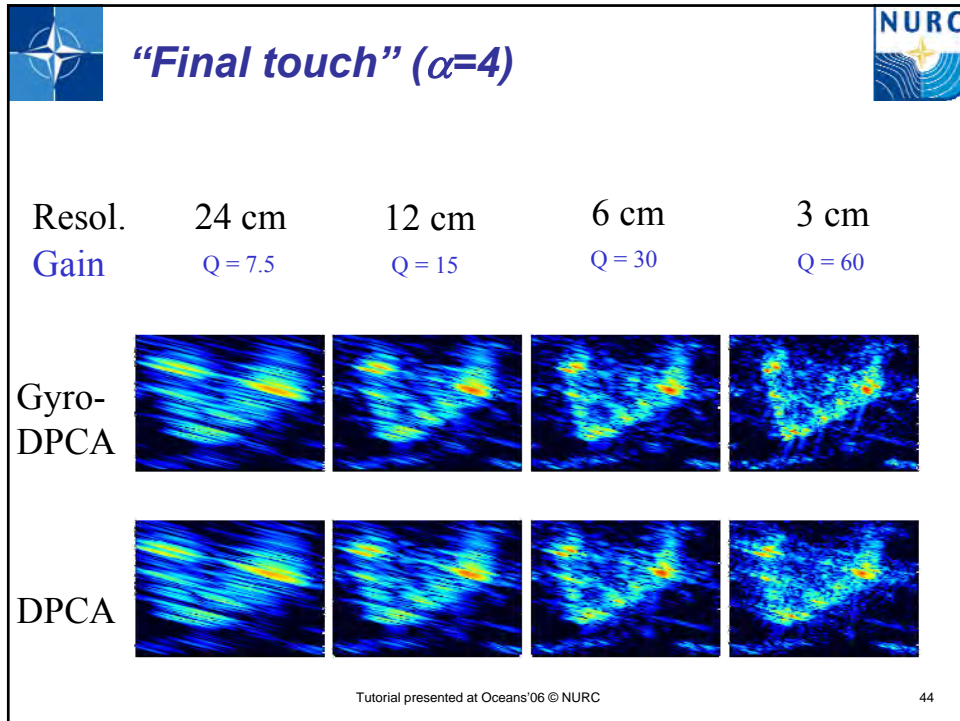
150 kHz
Bandwidth 60 kHz
26 cm length

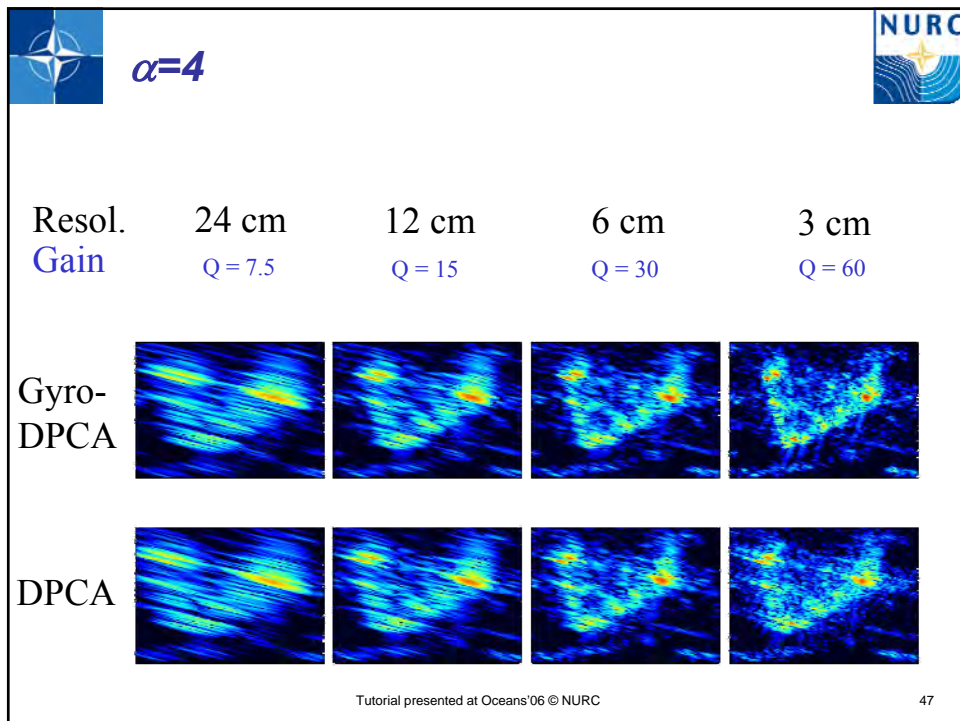
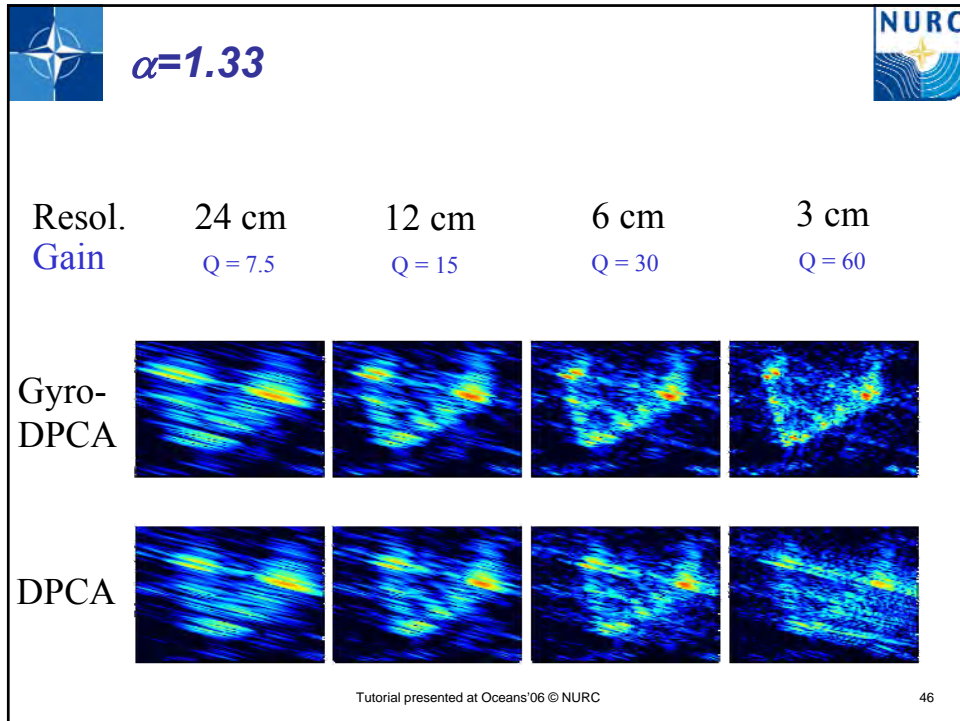
Tutorial presented at Oceans'06 © NURC

40





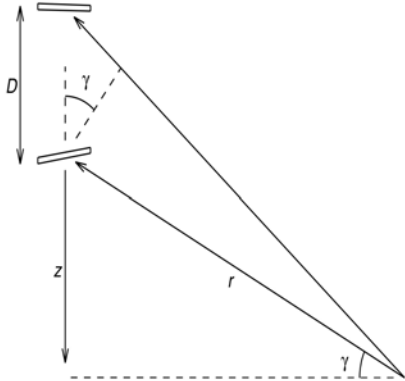






Grazing angle estimation using wideband interferometric sonar





- Two vertically superposed linear arrays separated by many wavelengths (>10).
- High accuracy local grazing angle estimation based on time delay estimation
- Similar in principle to DPCA with a physical across-track interferometer in place of a synthetic along-track interferometer.

Tutorial presented at Oceans'06 © NURC

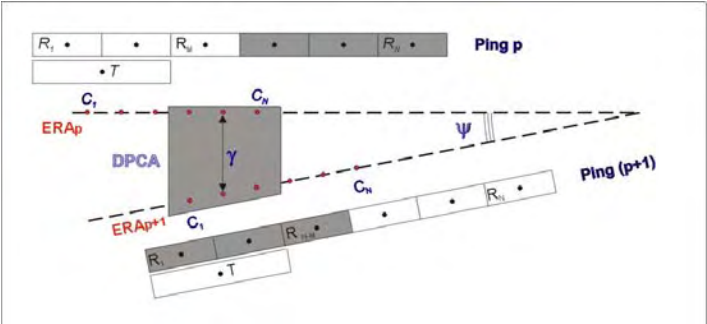
48



Along-track motion estimation



- The sonar can be slaved to the navigation system so that along-track ping-to-ping displacements are constant, effectively cancelling surge.
- Alternatively the DPCA can be extended to estimate the along-track displacement. The DPCA sway estimation is repeated for various DPCA lengths to retain the length for which the correlation is maximum (spatial interpolation requires $d < Lt$).



Tutorial presented at Oceans'06 © NURC

49



III. Shallow water operations

- Effect of multipath on micronavigated SAS
- Effect on SW fluctuations

Tutorial presented at Oceans'06 © NURC

50



Effect of multipath on DPCA correlation

- Multipath has been found experimentally to be a major factor degrading the ping-to-ping coherence of seafloor backscatter in shallow water.
- Multipath has negative impact on
 - Image contrast (shadow filling)
 - Interferometry performance (e.g. DPCA)
- Highlight structure is less affected due to large SAS array gain against ping-to-ping incoherent noise.

Tutorial presented at Oceans'06 © NURC

51



Multipath experiment





- 100 kHz array mounted vertically at 10.7 m depth in 20 m water depth
- 64 channel programmable transmitter array of length 48 cm
- 256 channel receiver array of length 192 cm.
- Bottom type: flat bottom of hard mud (Cinque Terre, Italy)
- Calm sea states

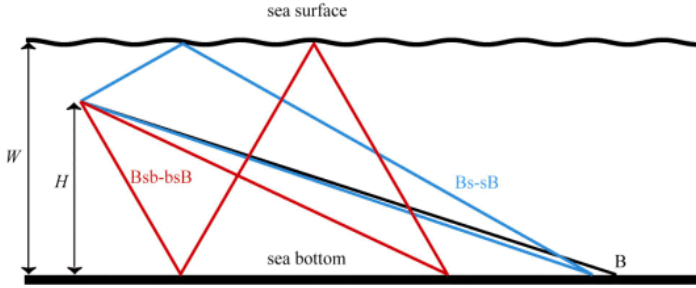
Tutorial presented at Oceans'06 © NURC

52



Multipath structure

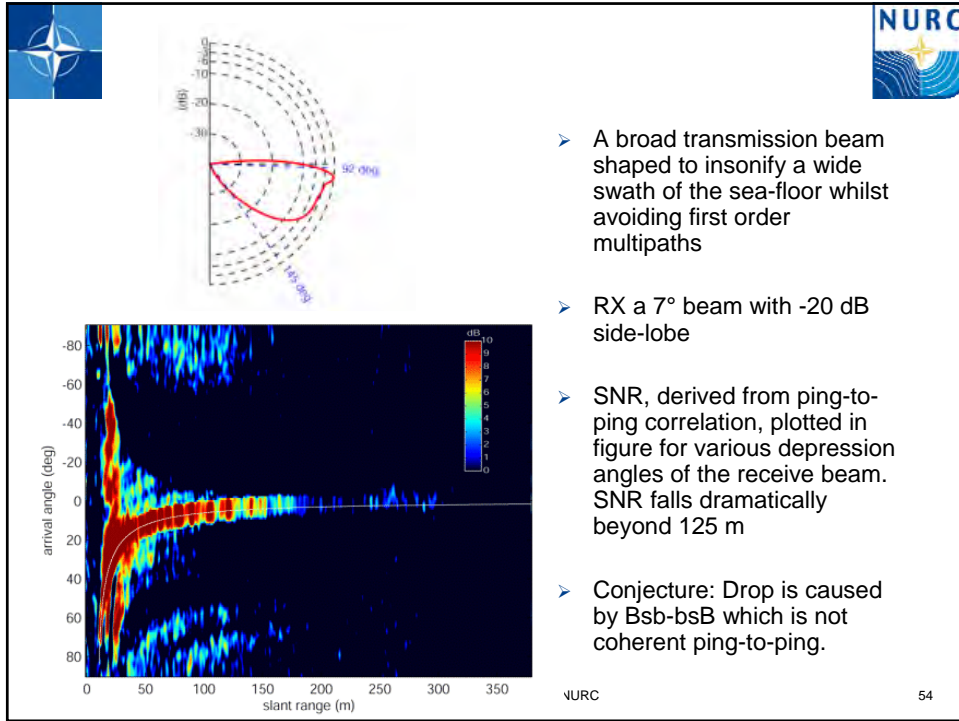




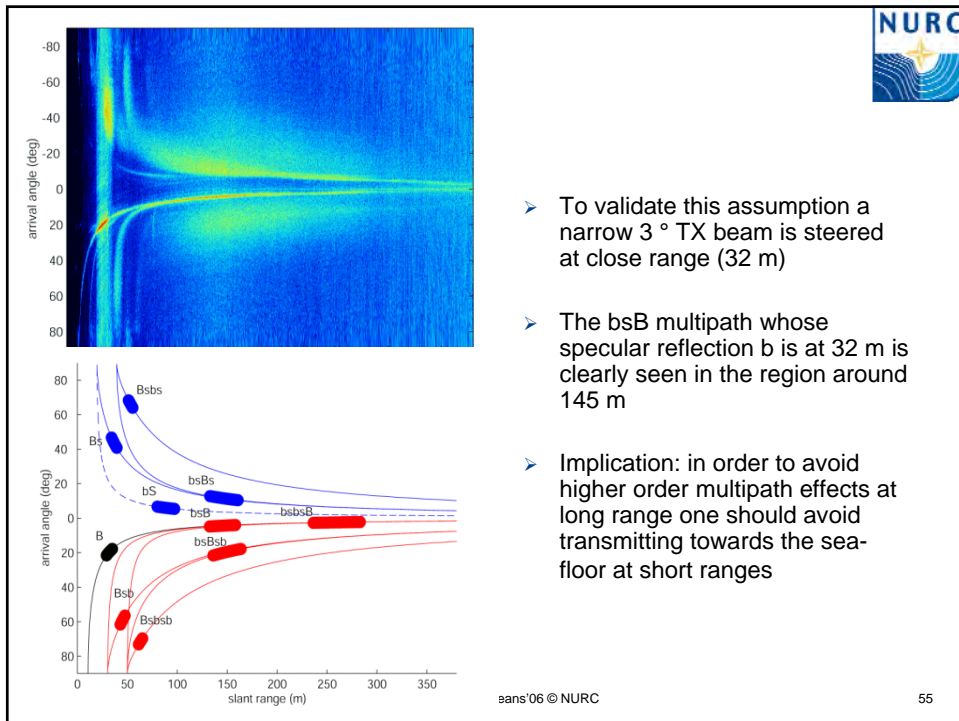
- Figure shows multipath interference of first order (B_s, sB) and second order (B_{sb}, bsB) arriving at the receiver at the same time as the direct path B.
- SW sonar performance can be expressed as a function of a generalised SNR, giving the ratio of the direct path B to multipath and noise.

Tutorial presented at Oceans'06 © NURC

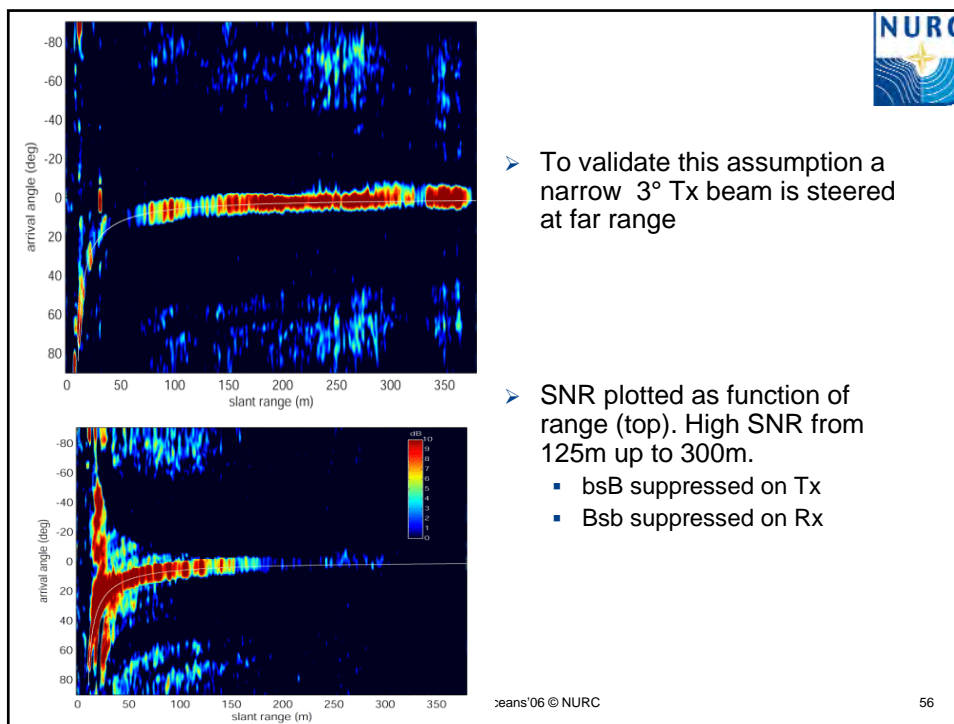
53



- A broad transmission beam shaped to insonify a wide swath of the sea-floor whilst avoiding first order multipaths
- RX a 7° beam with -20 dB side-lobe
- SNR, derived from ping-to-ping correlation, plotted in figure for various depression angles of the receive beam. SNR falls dramatically beyond 125 m
- Conjecture: Drop is caused by Bsb-bsB which is not coherent ping-to-ping.



- To validate this assumption a narrow 3° TX beam is steered at close range (32 m)
- The bsB multipath whose specular reflection b is at 32 m is clearly seen in the region around 145 m
- Implication: in order to avoid higher order multipath effects at long range one should avoid transmitting towards the sea-floor at short ranges



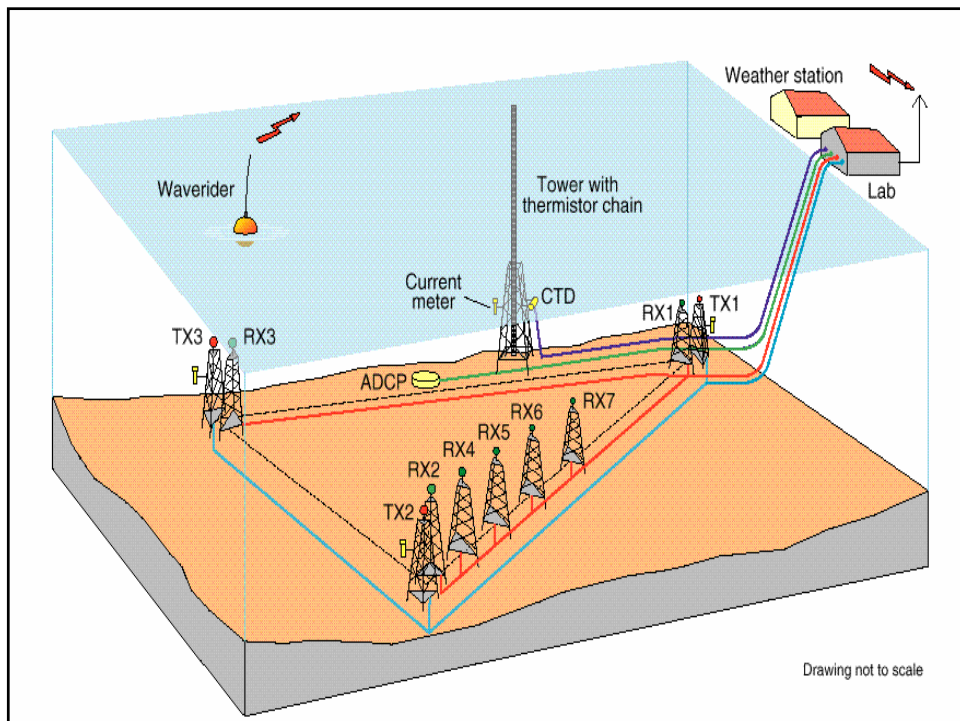
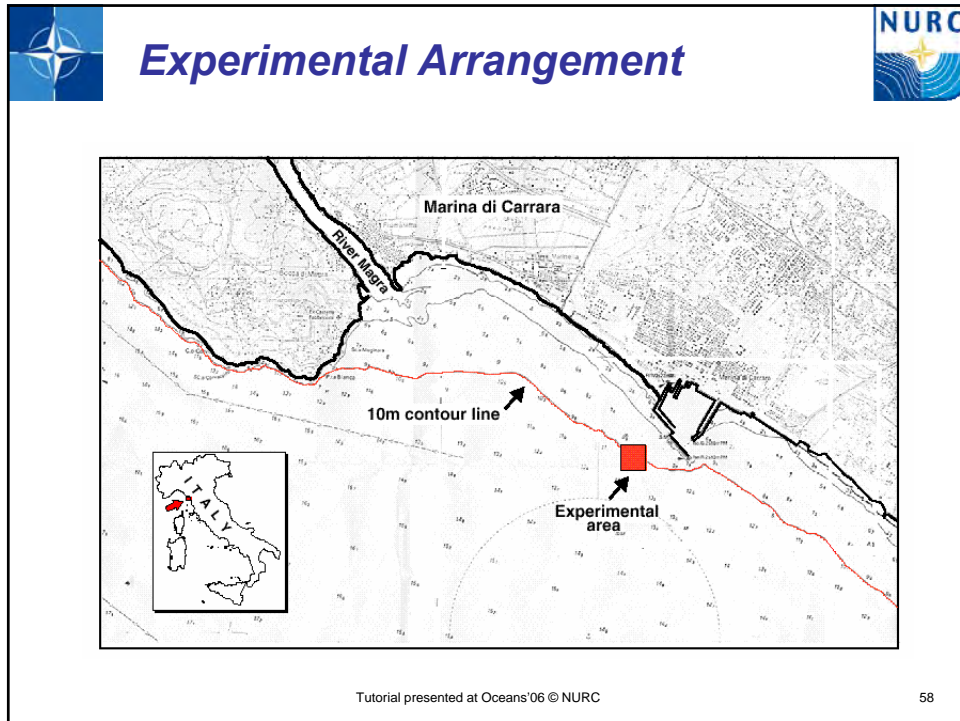
NURC

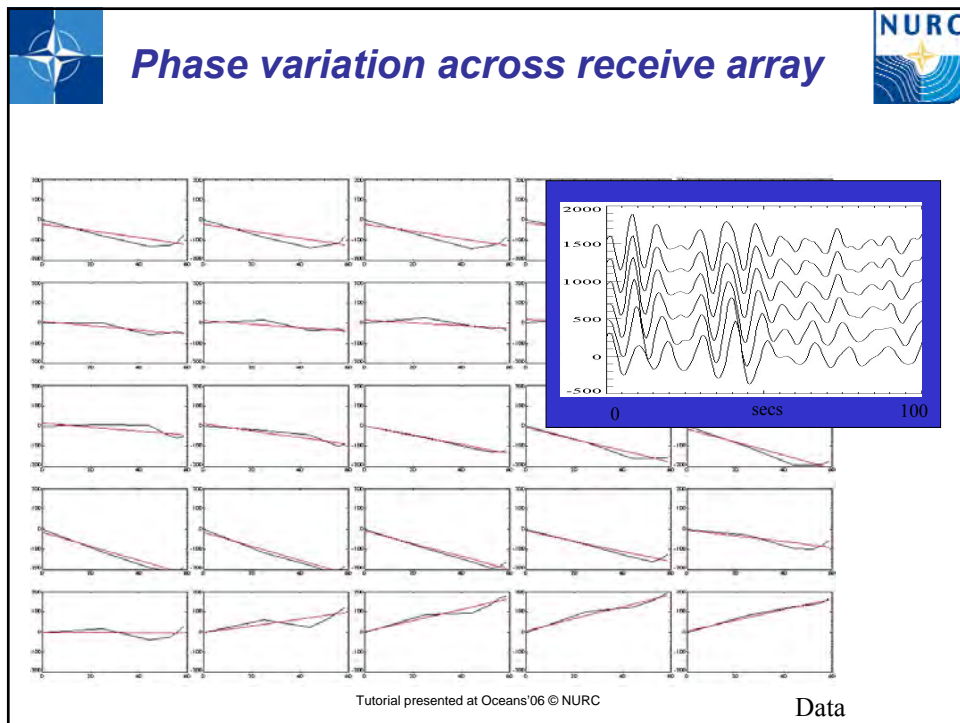
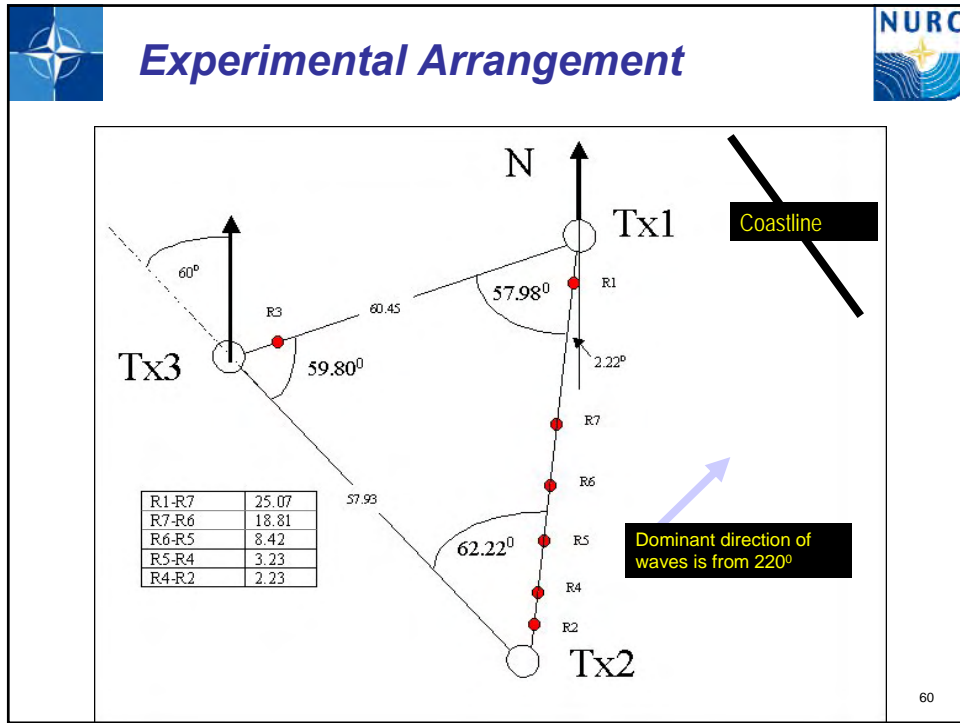
Effect of sea surface waves

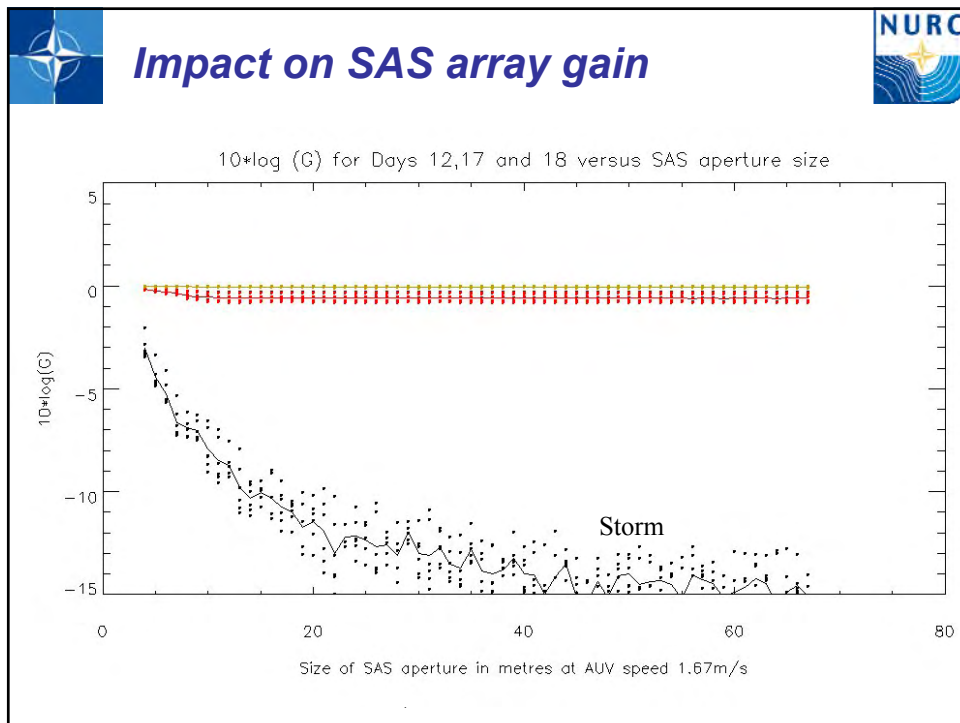
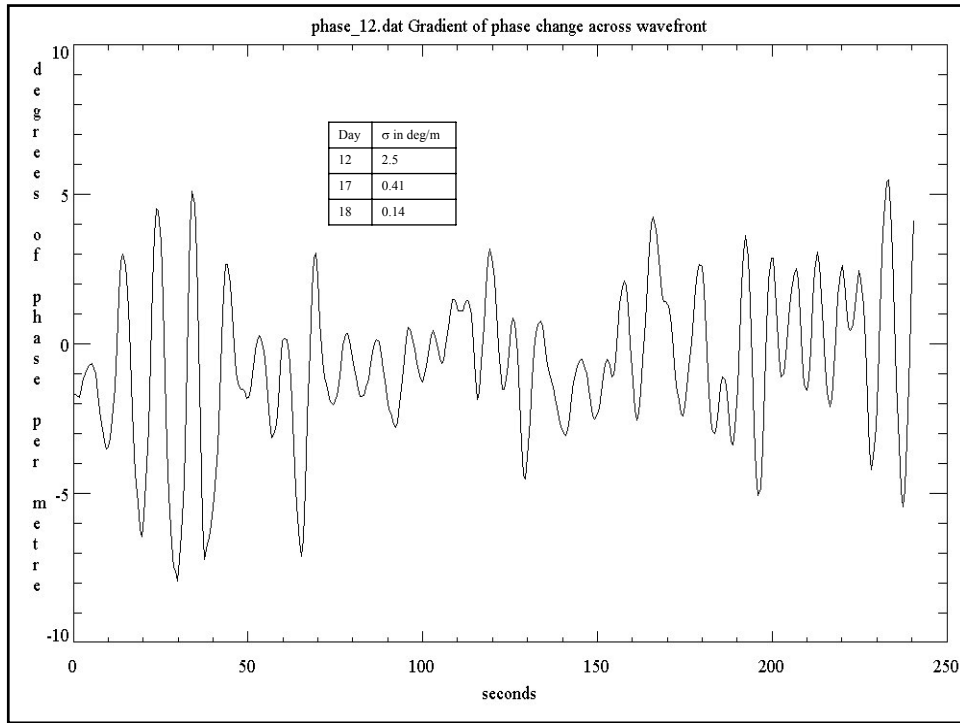
- Experiment arrangement
- Environmental data
- Data Examples
- Basis of model
- Comparison of data and model
- Impact on SAS

Tutorial presented at Oceans'06 © NURC

57









Findings of environmental study

- Phase variation across the ~60 m aperture at a range of ~60m from the transmitter TX3 is approximately linear in both calm and rough seas
- The temporal coherence function for the phase gradient is an oscillatory function and is driven by the sea surface wave spectrum.

Tutorial presented at Oceans'06 © NURC

64



IV. Applications

- Rail-based experiments
- Tow-body experiments
- AUV experiments

Tutorial presented at Oceans'06 © NURC

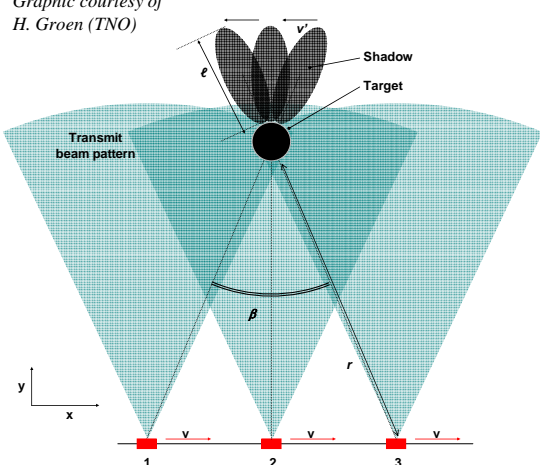
65



Shadow blur



Graphic courtesy of H. Groen (TNO)



- Excessive viewing angle differences at the extremities of the array lead to shadow blur
- This leads to a lower limit on the SAS resolution given by

$$CRR \geq \sqrt{\frac{\lambda l}{2}}$$

where l is the shadow length at the centre of the array

- Effect is minimized by increasing operating frequency.

Tutorial presented at Oceans'06 © NURC 66



SAS vs SSS images of a wreck



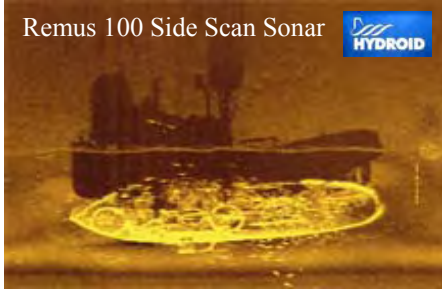
Remus 600 HF Synthetic Aperture Sonar





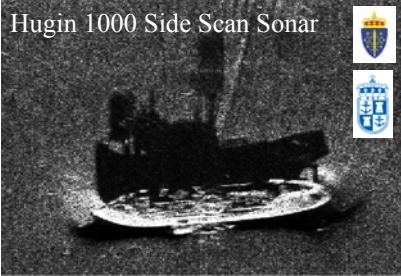


Remus 100 Side Scan Sonar



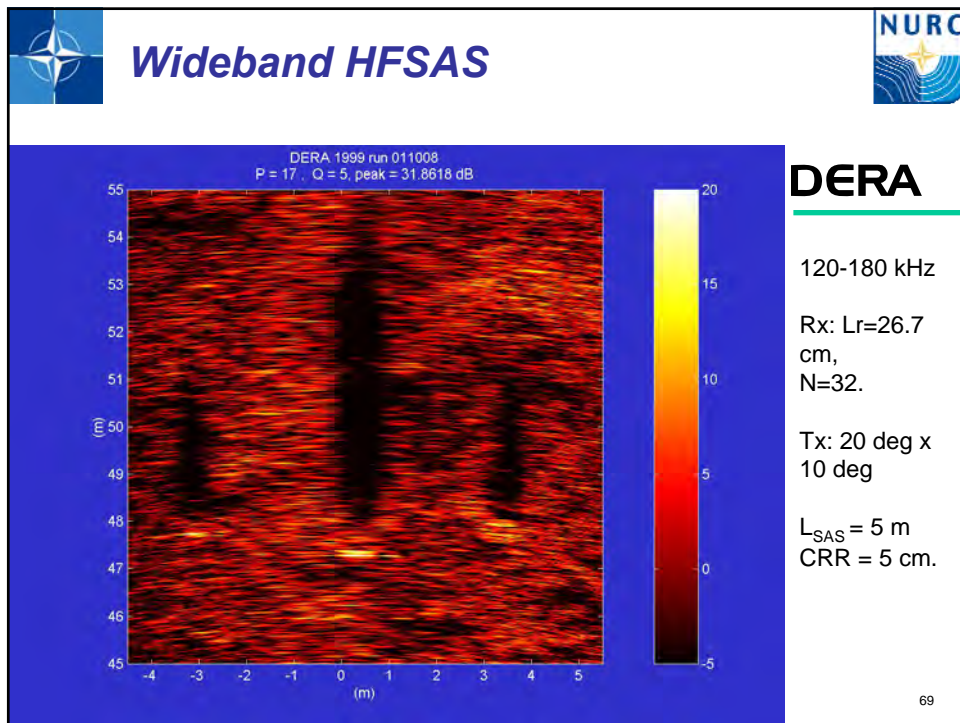
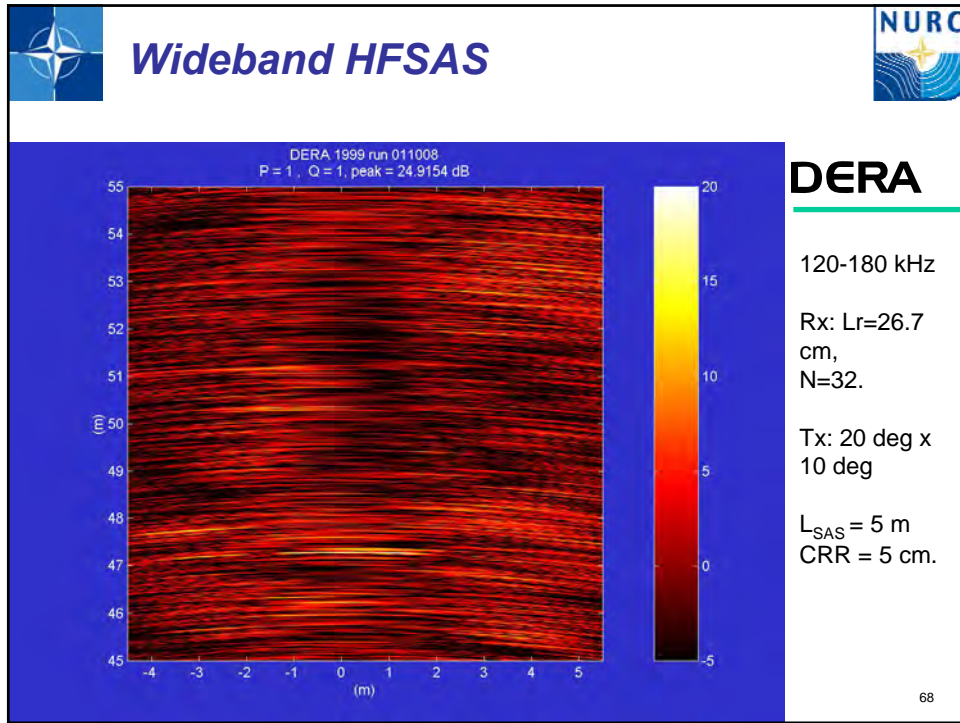


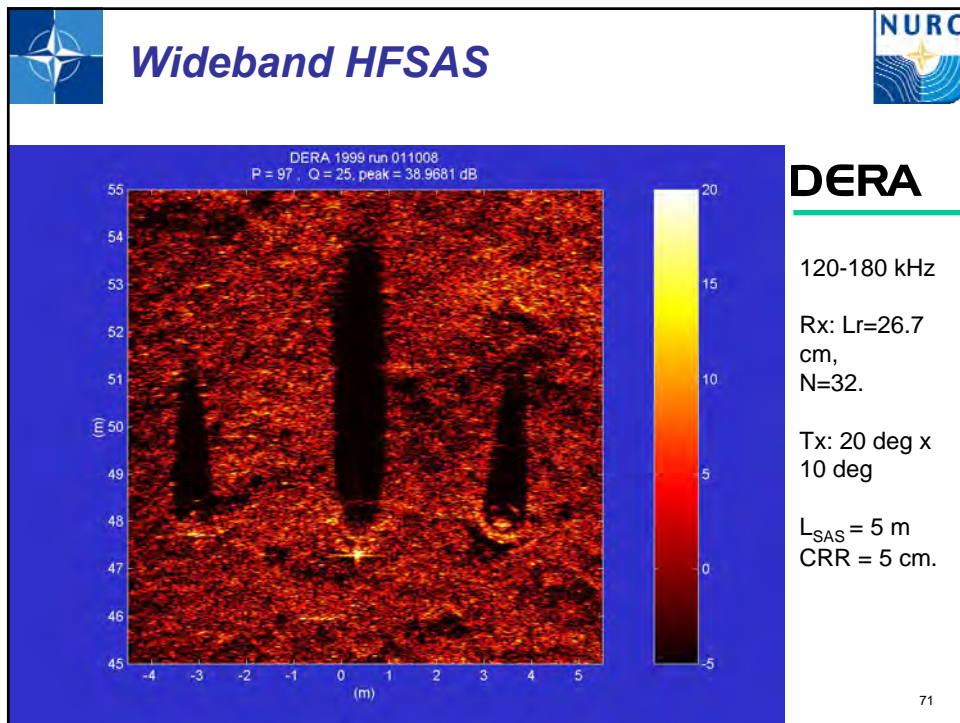
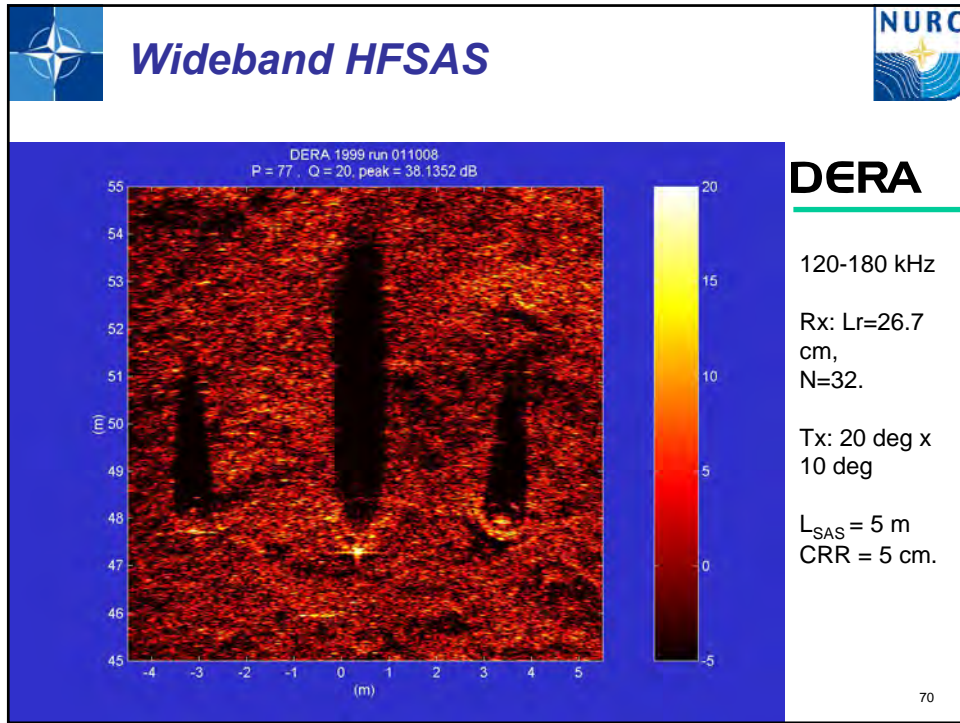
Hugin 1000 Side Scan Sonar

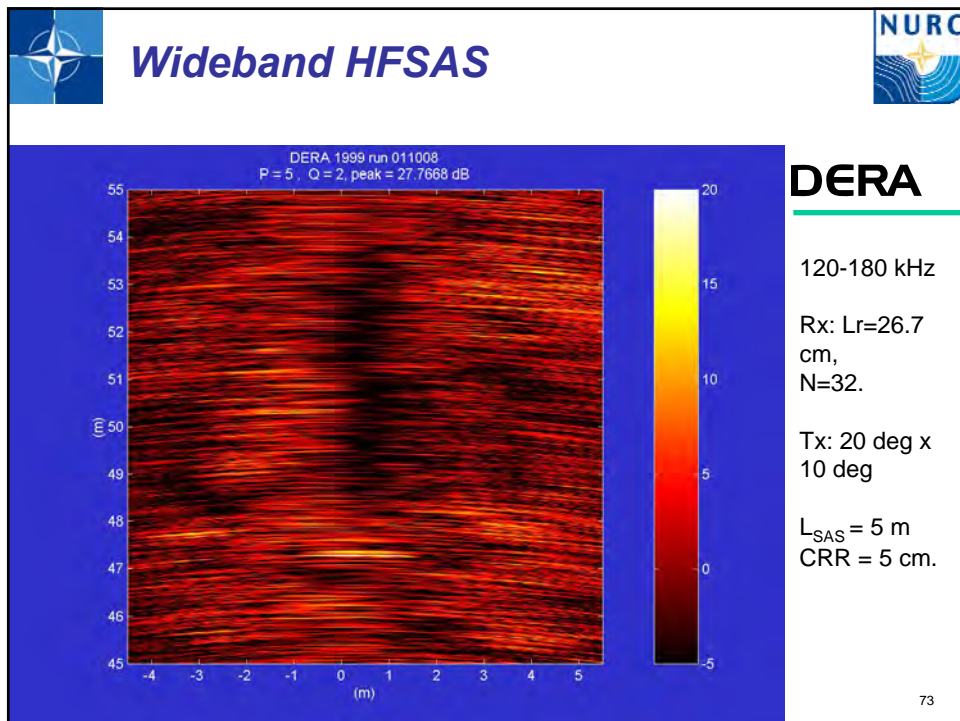
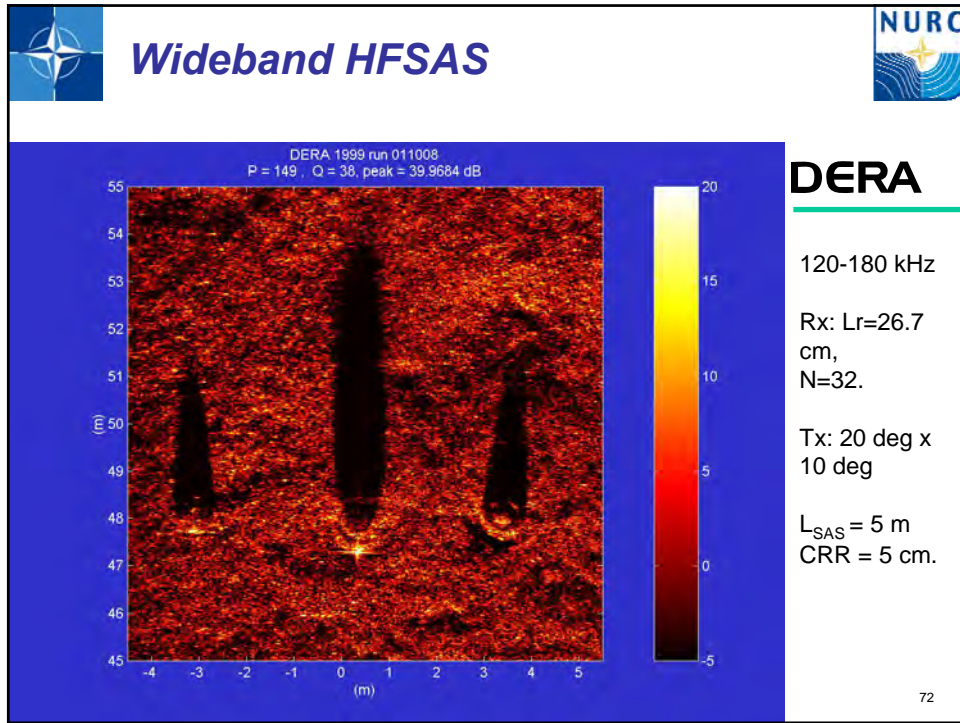


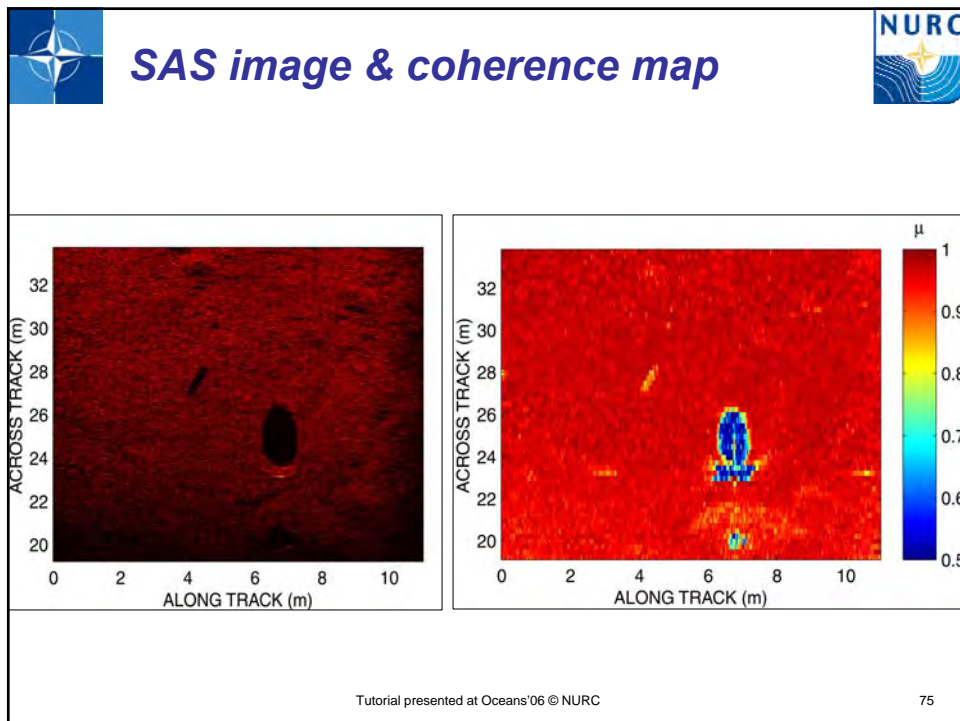
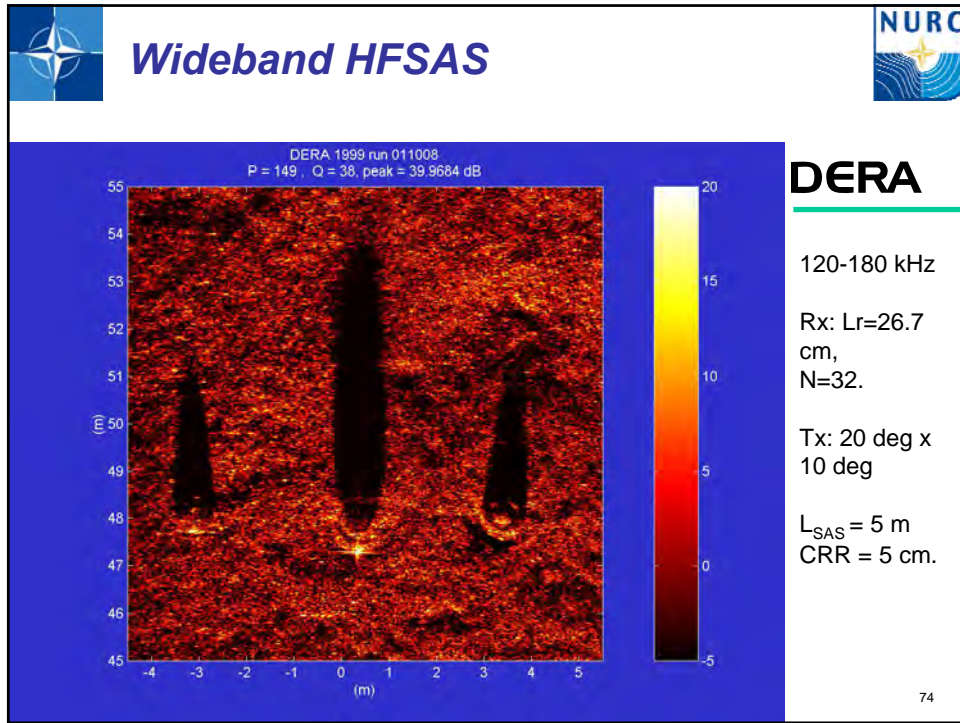


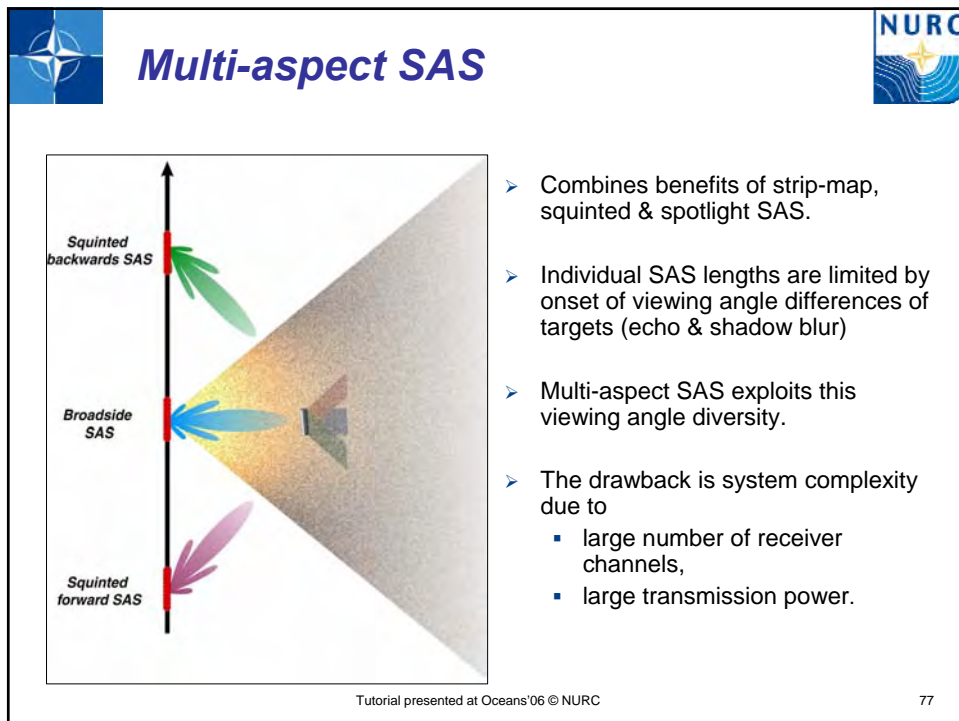
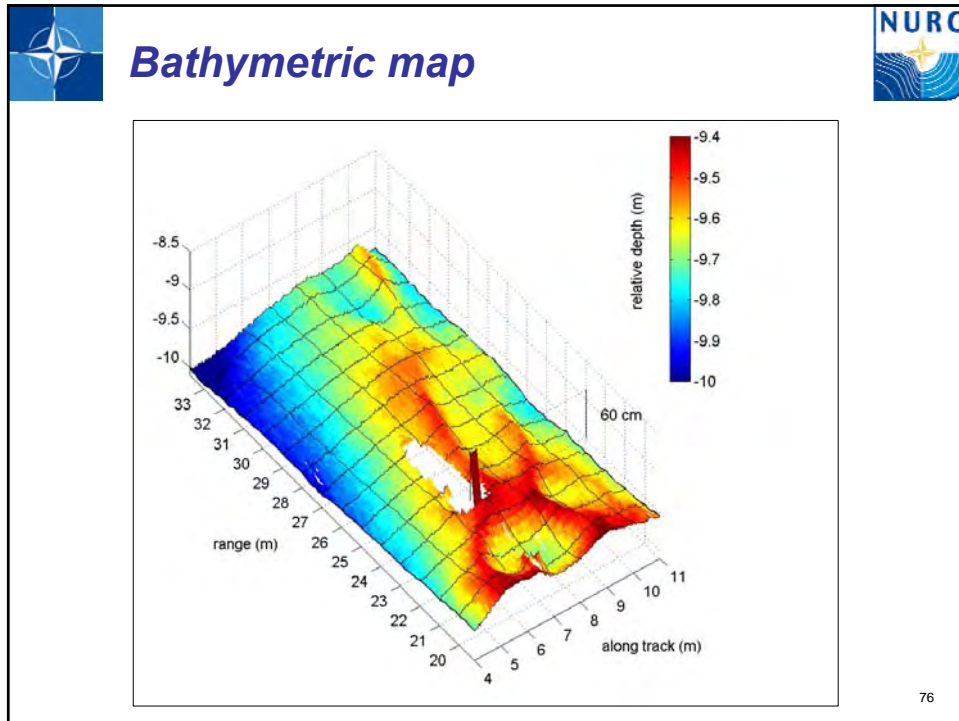

Tutorial presented at Oceans'06 © NURC 67



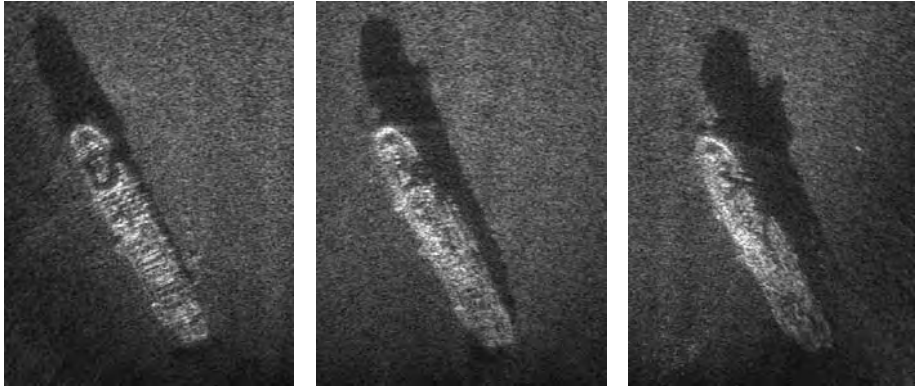








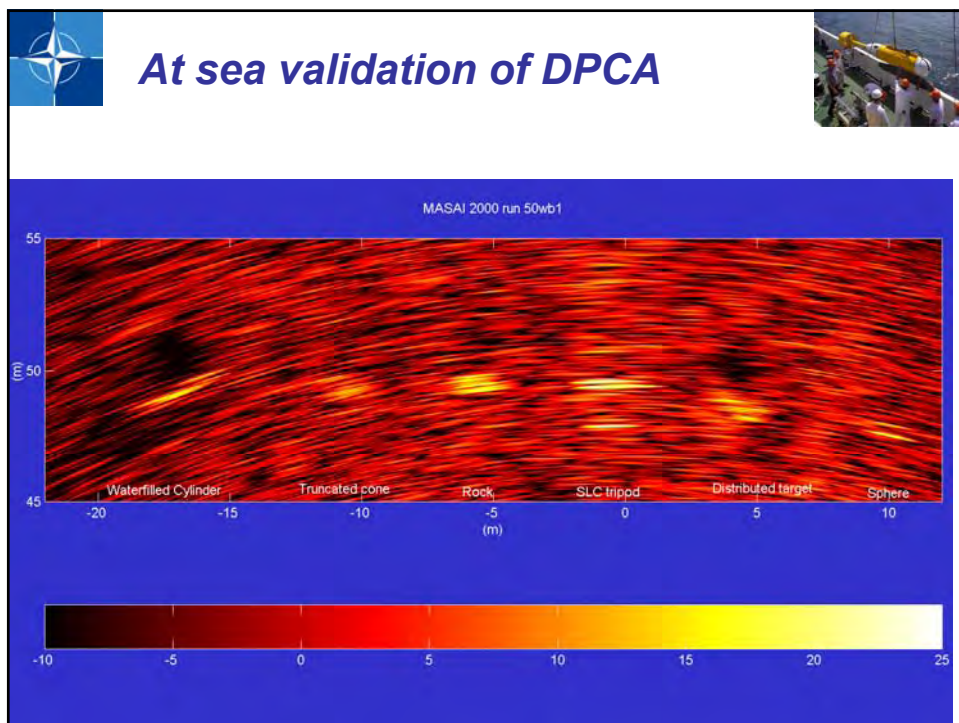
 **100kHz multi-aspect imaging** 

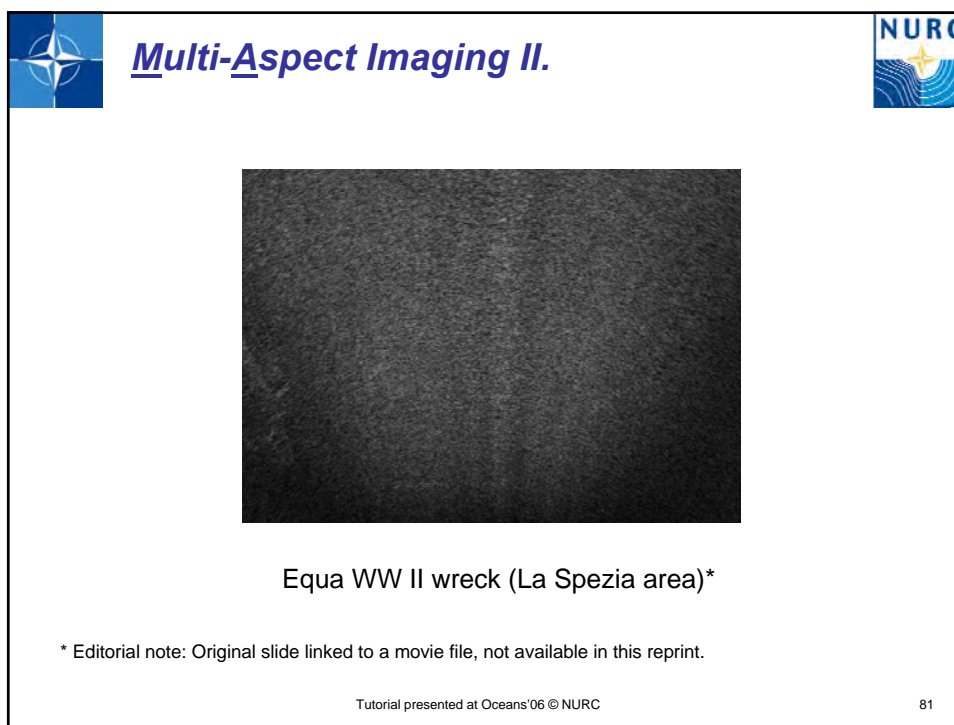
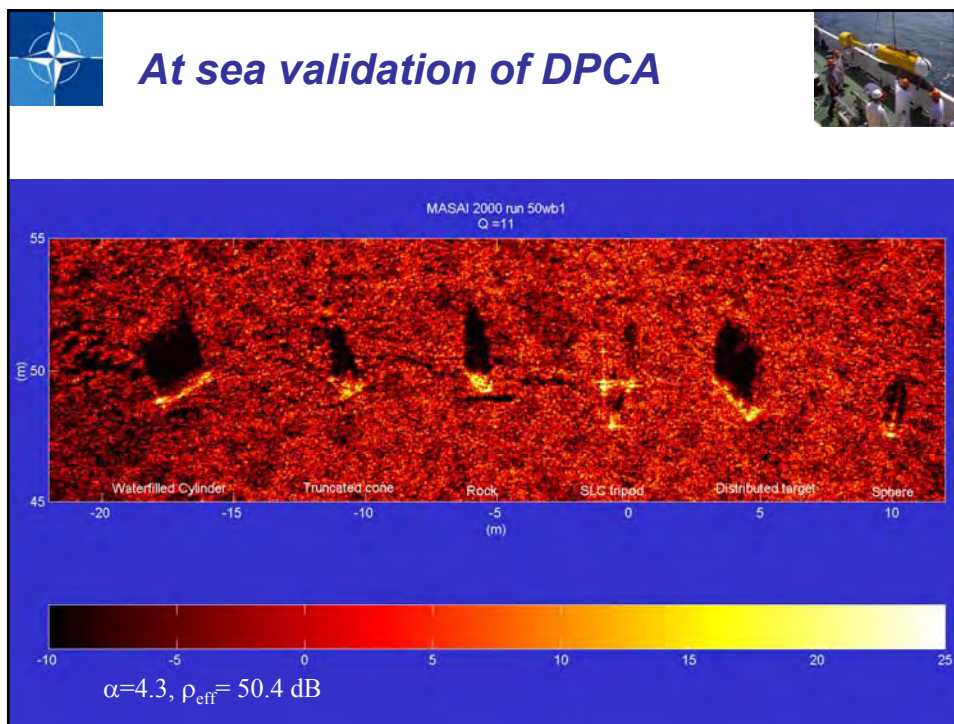


Equa WW II wreck (La Spezia area)

Tutorial presented at Oceans'06 © NURC

78

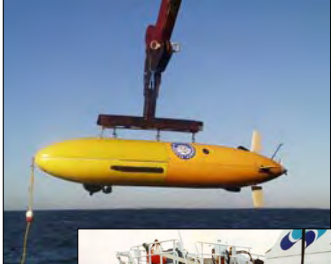






AUV based Synthetic Aperture Systems






Ocean Explorer AUV

- AUVs are the future of commercial and military seafloor surveys

- AUVs are well suited to SAS:
 - operate at low speeds (3-4 knots) for endurance
 - equipped with high performance navigation
 - good stability independent of sea state

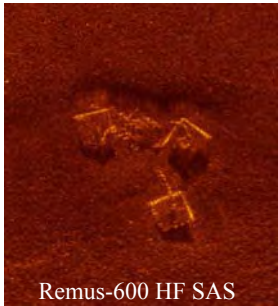
- Major collaborative R&D program on-going at Saclantcen which includes AUV-based SAS

Tutorial presented at Oceans'06 © NURC 82



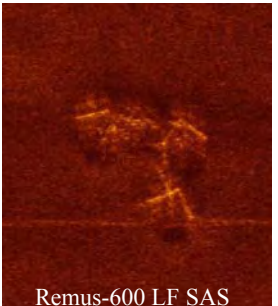
Examples of Synthetic Aperture Sonar and Side Scan Sonar





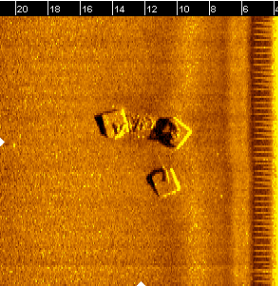
20 m
25 m

Remus-600 HF SAS



20 m
25 m

Remus-600 LF SAS



20 18 16 14 12 10 8 6 4

Remus-100 MS 900kHz SSS



70 m
65 m

Hugin EdgeTech 4400 SAS

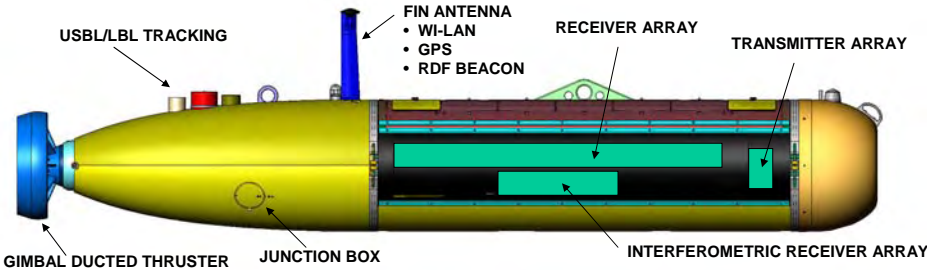
Tutorial presented at Oceans'06 © NURC 83



MUSCLE



- Compact (3.5 m) and lightweight (400 kg) 21" vehicle (Bluefin)
- High accuracy (<5 m/hr) IXSEA PHINS aided inertial navigation system
- Real-time multi-beam SSS (13 beams spaced at 4 cm)
 - Programmable transmission with down to 2 deg beam width
 - Long range and short range transmissions in two sub-bands
 - Receive elements with selectable vertical beampatterns
- Plan to implement on-board SAS processing up to 2.5 cm at 225m

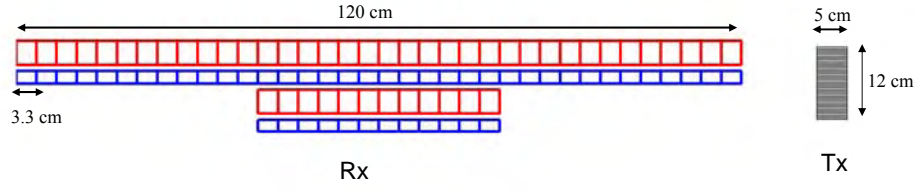


Tutorial presented at Oceans'06 © NURC



NATO SONAR DESIGN

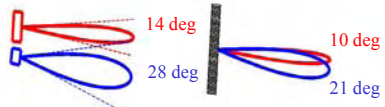




Long-range: Red frequency (270-300 kHz), Narrow-beam Tx/Rx with 4 deg depression

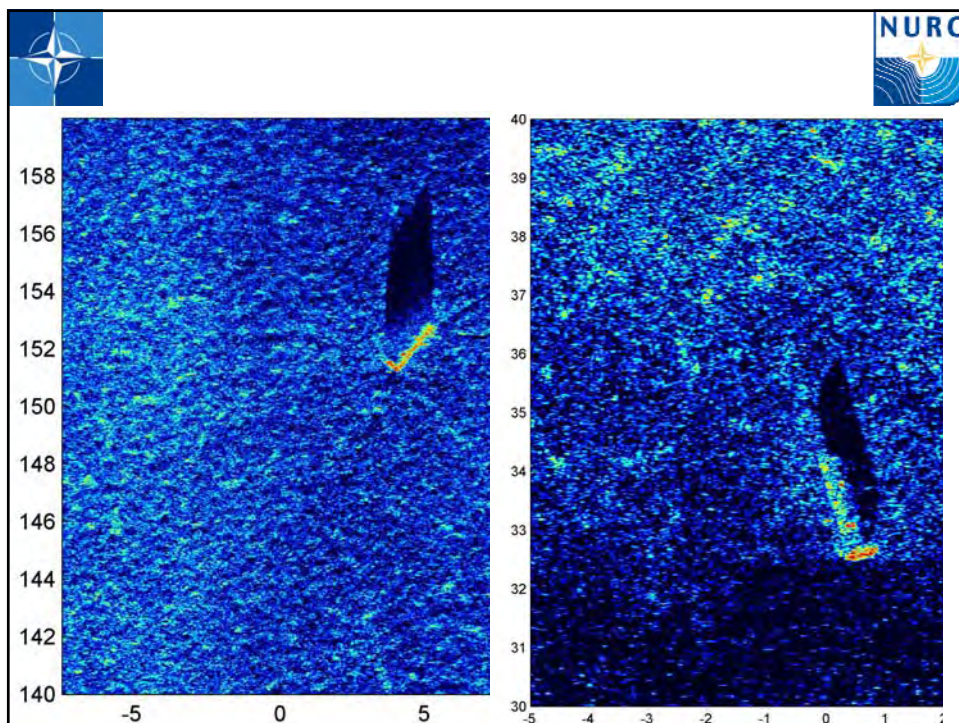
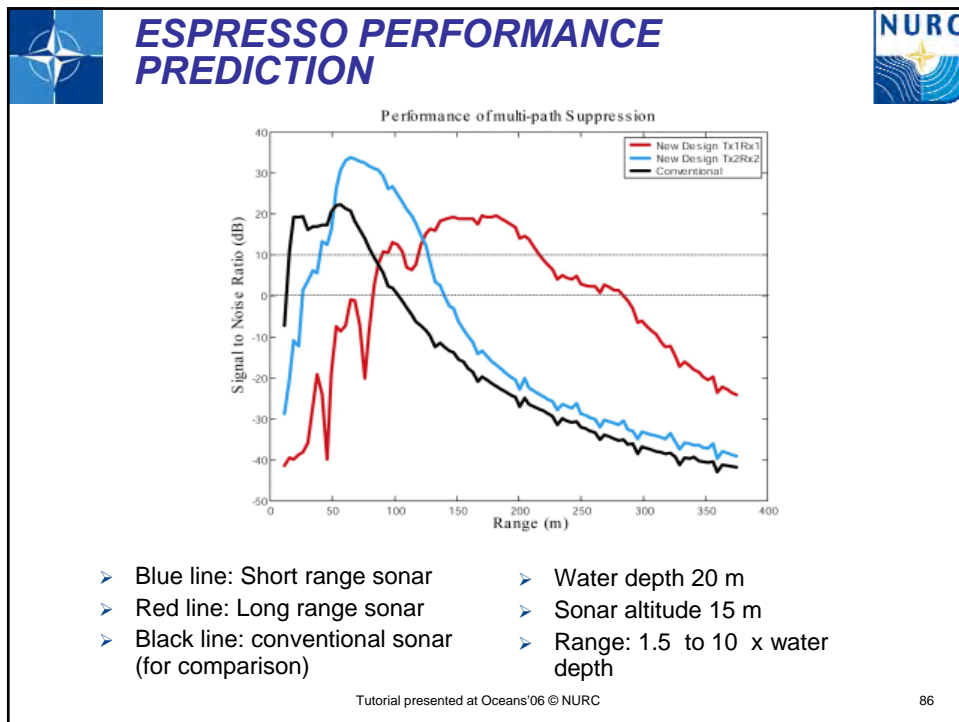
Short range: Blue frequency (300-330 kHz), Wide-beam Tx/ Rx with 8 deg depression

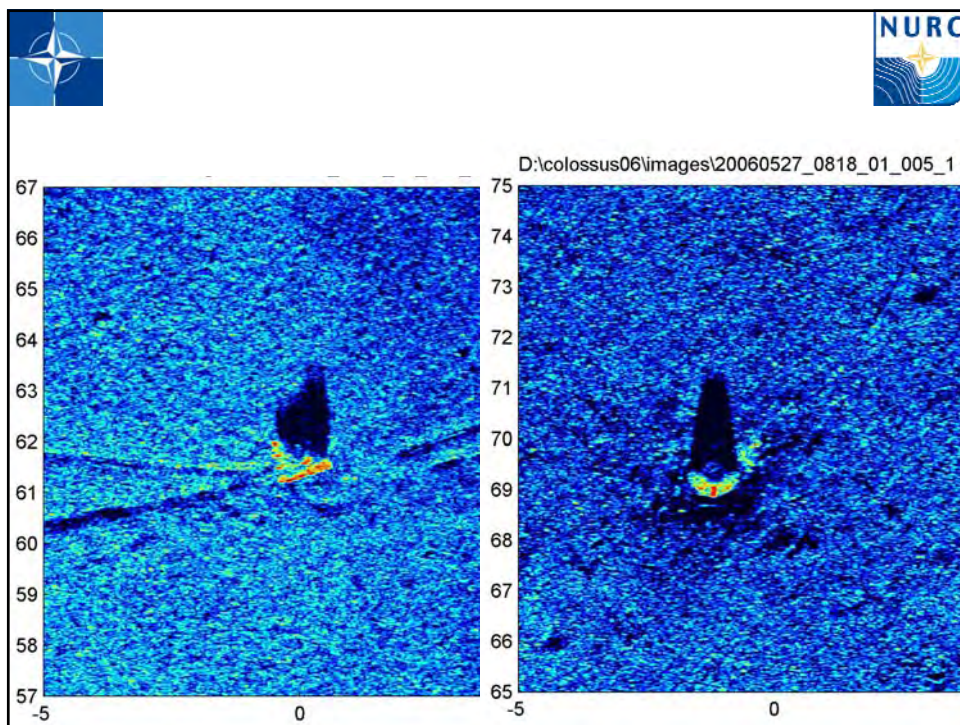
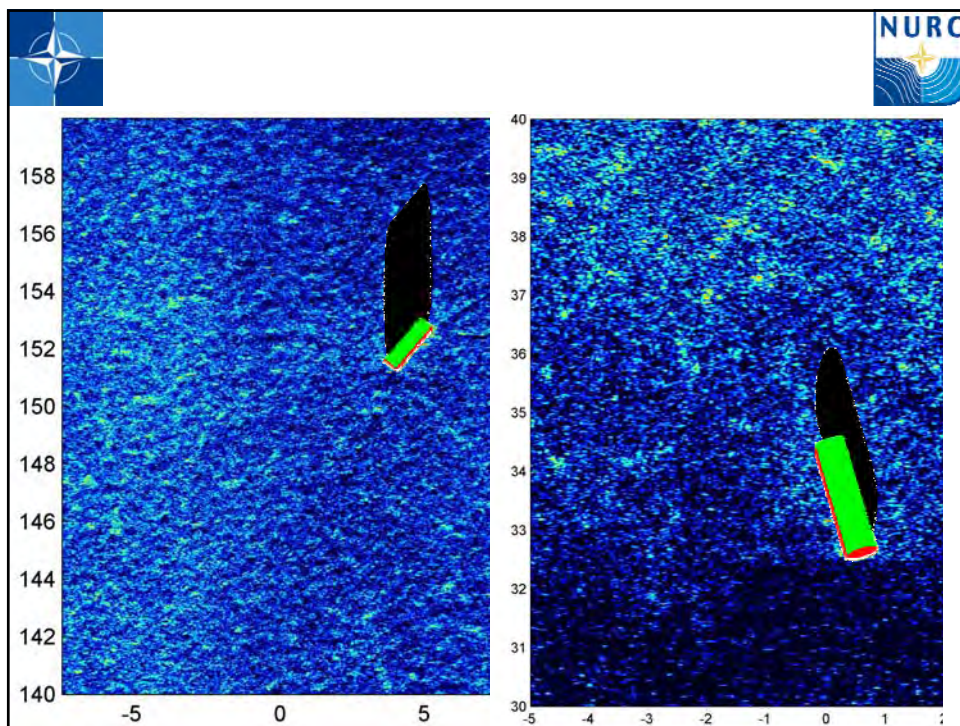
Multipath is rejected by a combination of spatial & temporal filtering

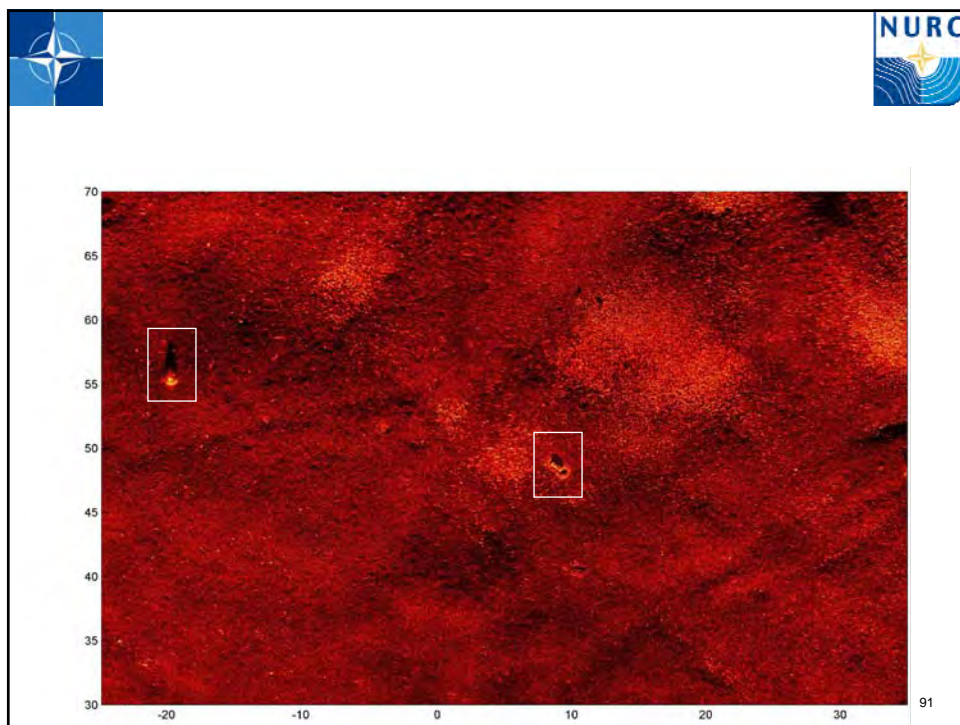
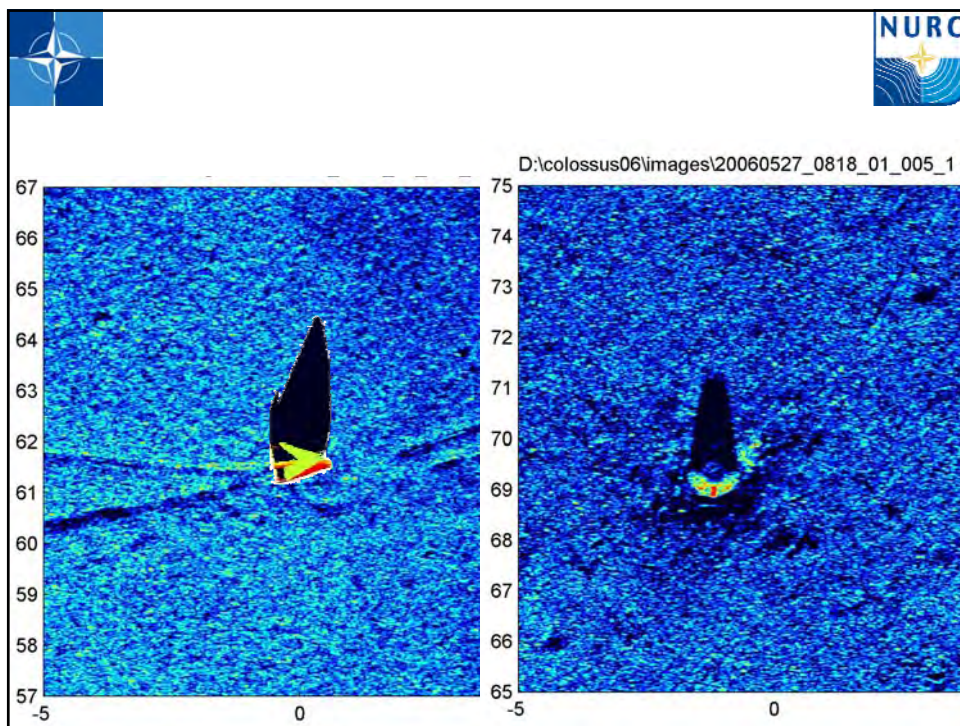


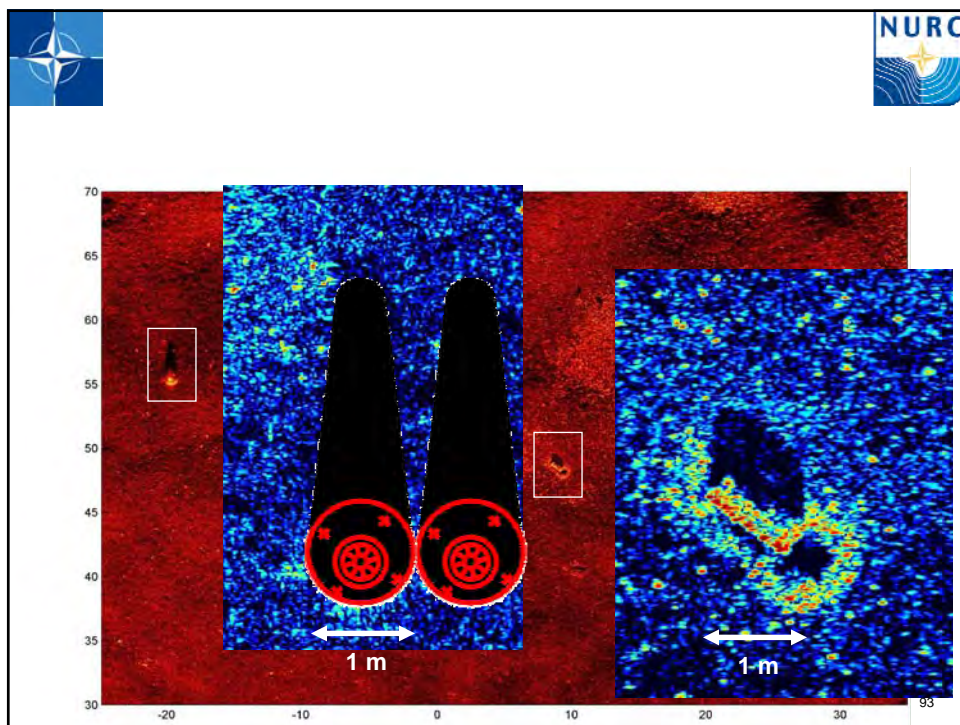
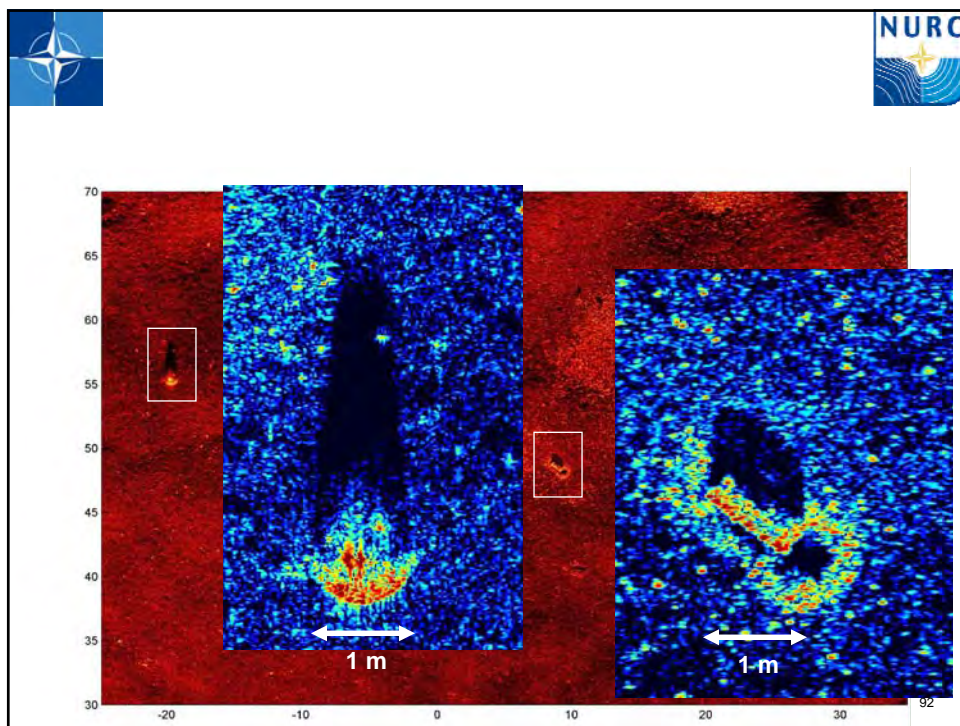
Tutorial presented at Oceans'06 © NURC

85









Document Data Sheet

<i>Security Classification</i> RELEASABLE TO THE PUBLIC		<i>Project No.</i>
<i>Document Serial No.</i> NURC-PR-2006-029	<i>Date of Issue</i> October 2006	<i>Total Pages</i> 52pp.
<i>Author(s)</i> Pinto, Marc		
<i>Title</i> Design of synthetic aperture sonar systems for high-resolution seabed imaging (tutorial slides)		
<i>Abstract</i> .		
<i>Keywords</i>		
<i>Issuing Organization</i> NATO Undersea Research Centre Viale San Bartolomeo 400, 19138 La Spezia, Italy [From N. America: NATO Undersea Research Centre (New York) APO AE 09613-5000]		Tel: +39 0187 527 361 Fax: +39 0187 527 700 E-mail: library@nurc.nato.int